doi:10.1038/nature09634

Supplementary Figures

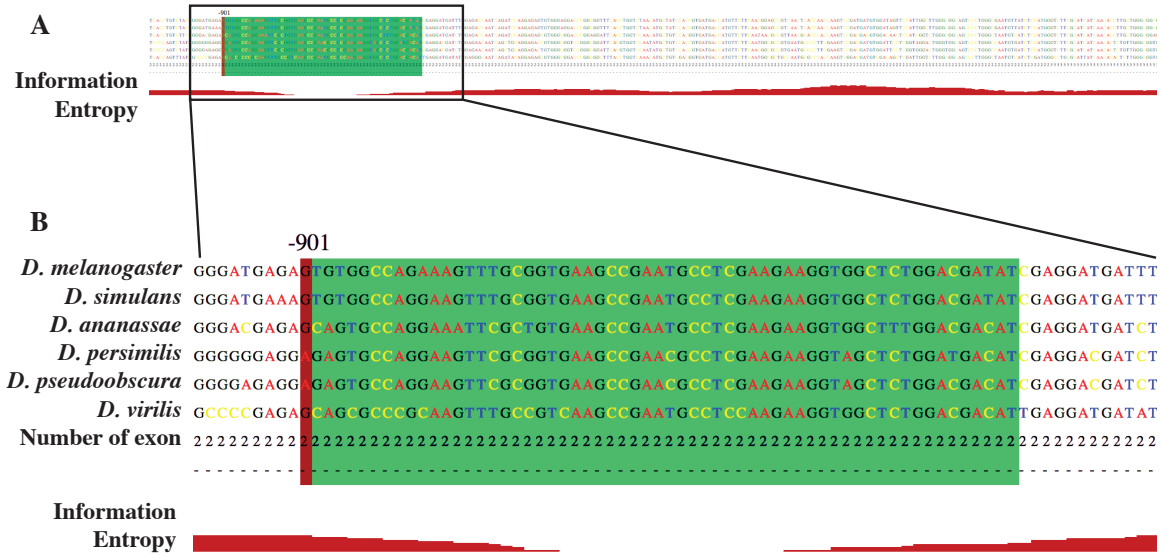

Supplementary Figure 1. Finding conserved sequences in orthologous transcripts of six *Drosophilidae* aligned relative to *D. melanogaster*. **a**, Entropy landscape (red track) in the second exon of *D. melanogaster* gene *CG4702* and its five orthologs. Green box represents one 60nt long window. **b**, Zoom into an entropy valley. The candidate probe (green box) is located in a region of the lowest entropy; its initial nucleotide is marked with red.

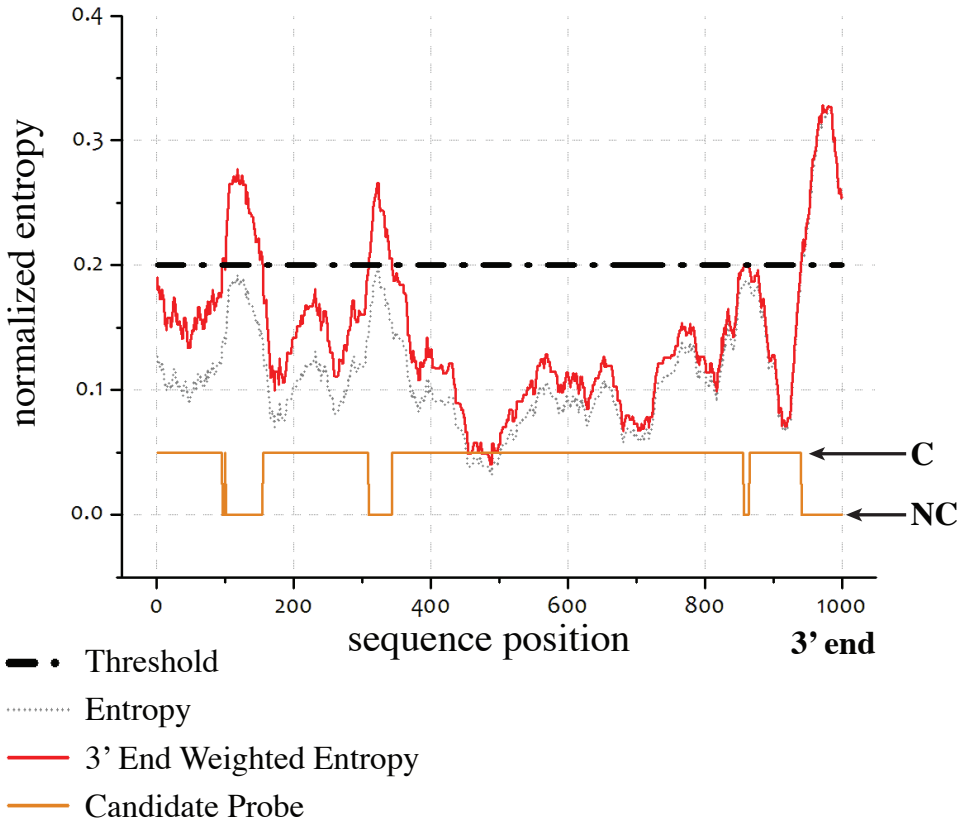

Supplementary Figure 2. Plot of information entropy in the 1kb region at the 3′ end of the transcript of the gene *CG4702*. The yellow Candidate Probe track shows regions considered **(C)** and not considered **(NC)** for probe design.

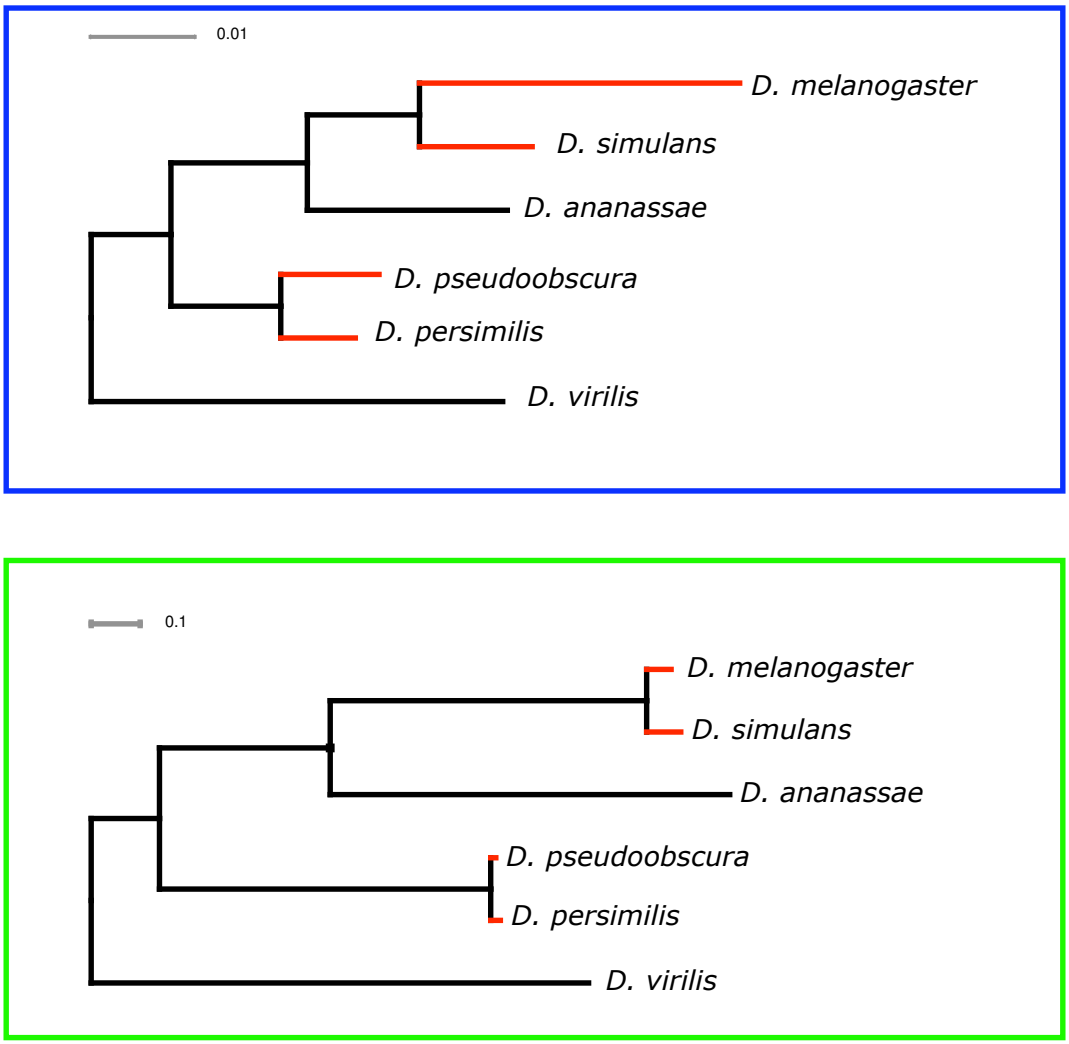

Supplementary Figure 3. A comparison of the phylogenetic relationships between the six *Drosophila* species used in our study when drawn up using our gene expression data (based on normalised values from a linear model (see Methods)) - boxed in blue - and based on median dS values for $\sim 10,000$ orthologous genes - boxed in green. Red branches indicate terminal branches between sister species that are longer in the gene expression data.

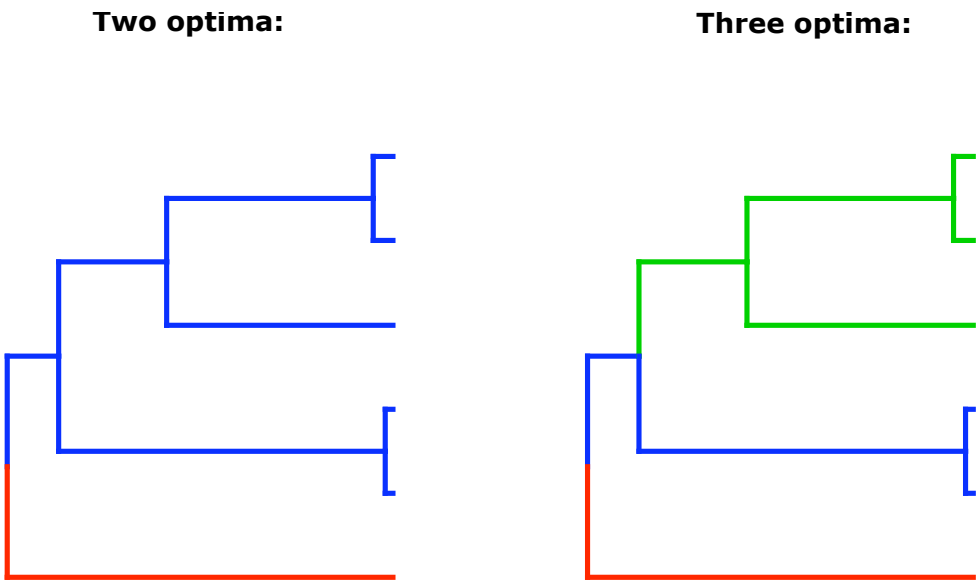

Supplementary Figure 4. Two different evolutionary scenarios whereby directional selection produces new stabilising selection optima along different branches of the phylogeny. Species at the tips are ordered from top to bottom: *D. melanogaster*, *D. simulans*, *D. ananassae*, *D. pseudoobscura*, *D. persimilis*, and *D. virilis*.

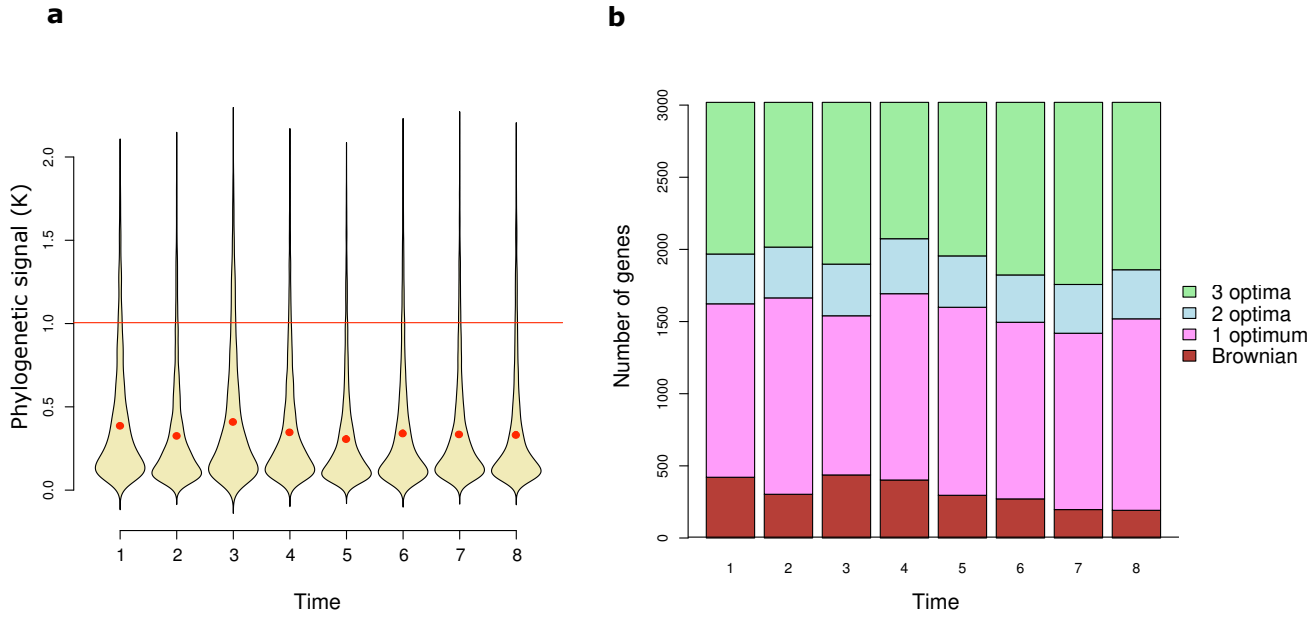

Supplementary Figure 5. Stabilising selection best explains gene expression evolution during *Drosophila* embryogenesis. **a**, Violin plots showing the distributions of phylogenetic signal at each time point for GST values. Values less than 1 indicate a weaker phylogenetic signal than phylogenies produced by a Brownian evolutionary process. Red circles indicate the mean, and the red line marks a phylogenetic signal of 1. **b**, The number of genes that fit best to one of four different evolutionary models at each time point.

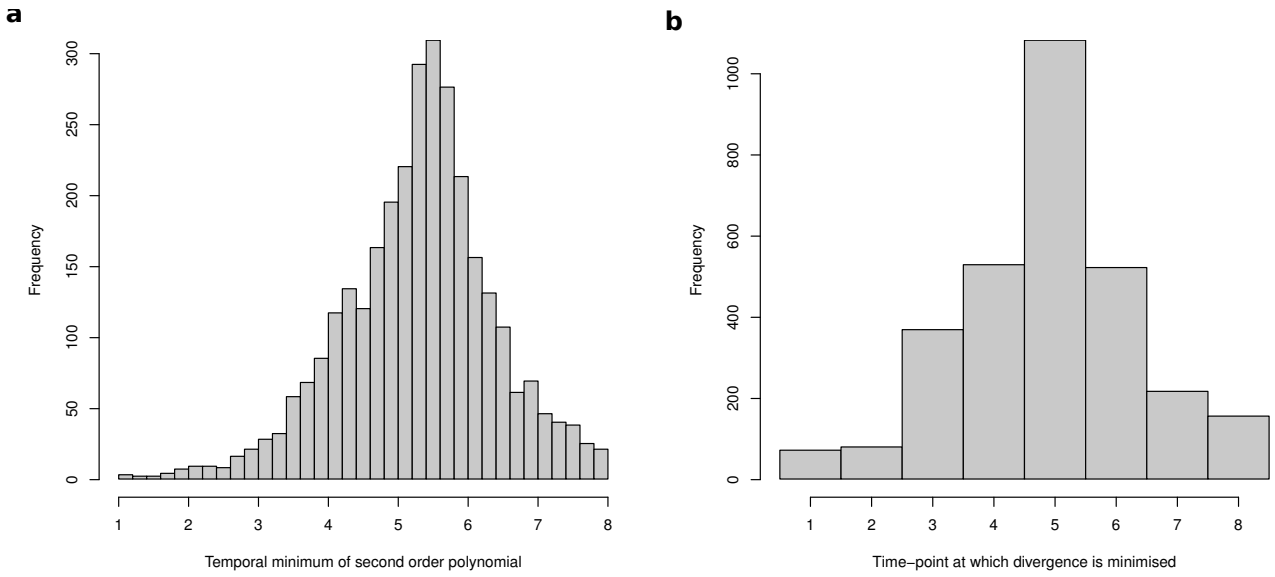

Supplementary Figure 6. The time points at which temporal divergence is minimised per gene according to, **a**, the minima of second order polynomials fitted to each gene's divergence profile, and **b**, the time point at which divergence is lowest for each gene's divergence profile. The plots show that the hourglass divergence profile seen across the dataset is seen on a gene-by-gene basis also, rather than being a composite of genes with high divergence early and genes with high divergence late.

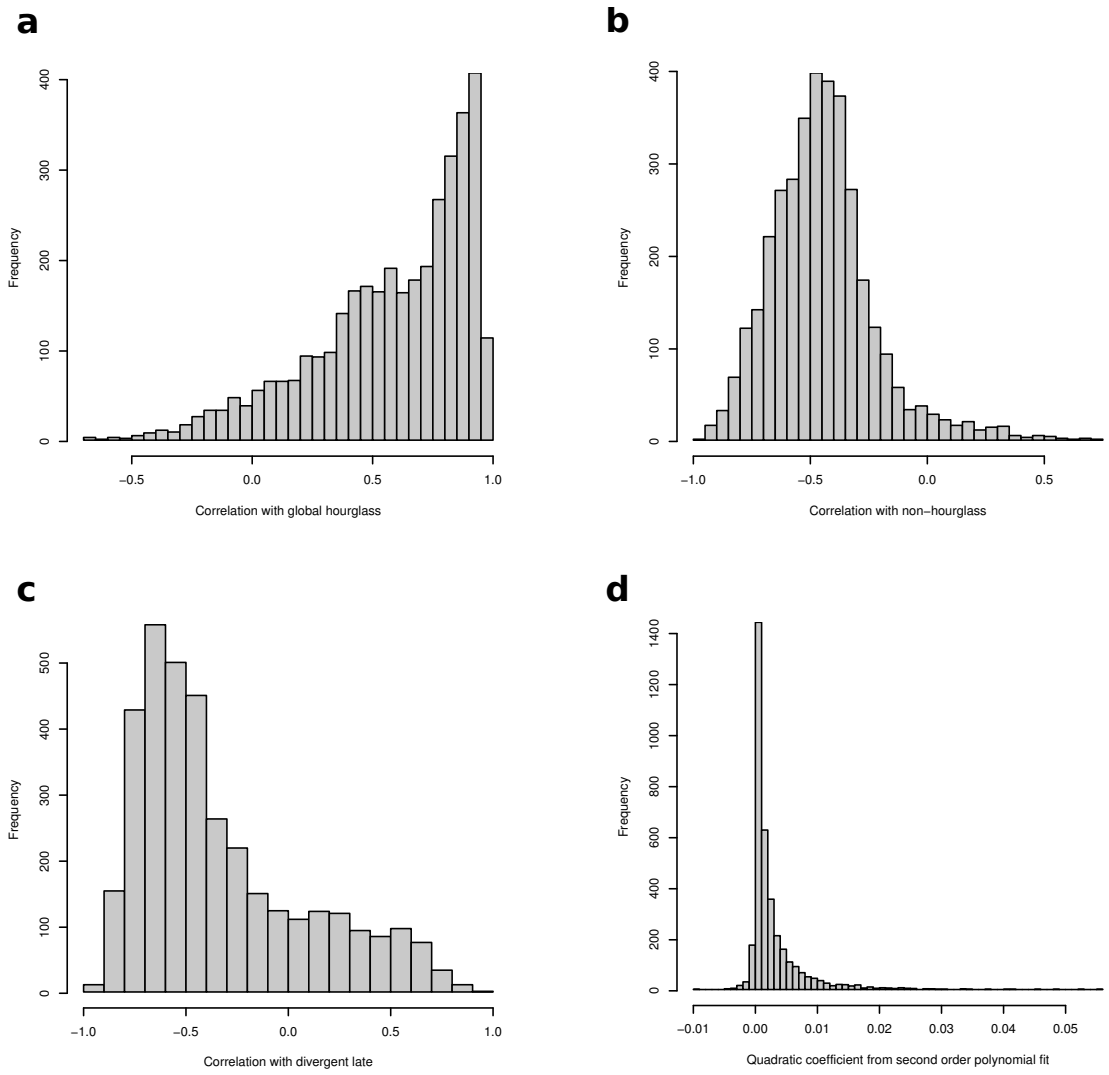

Supplementary Figure 7. The distribution of divergence profile correlations for individual genes with **a**, the global hourglass divergence profile, **b**, a divergence profile that peaks at time points 4, 5, and 6, **c**, a linearly increasing divergence profile, and **d**, the distribution of quadratic coefficients from second order polynomial fits to each gene's divergence profile showing that the majority of genes fit profiles with minima (positive coefficients). The distributions show that most genes correlate positively with an hourglass divergence profile, whereas far fewer genes correlate positively with non-hourglass or increasing divergence profiles.

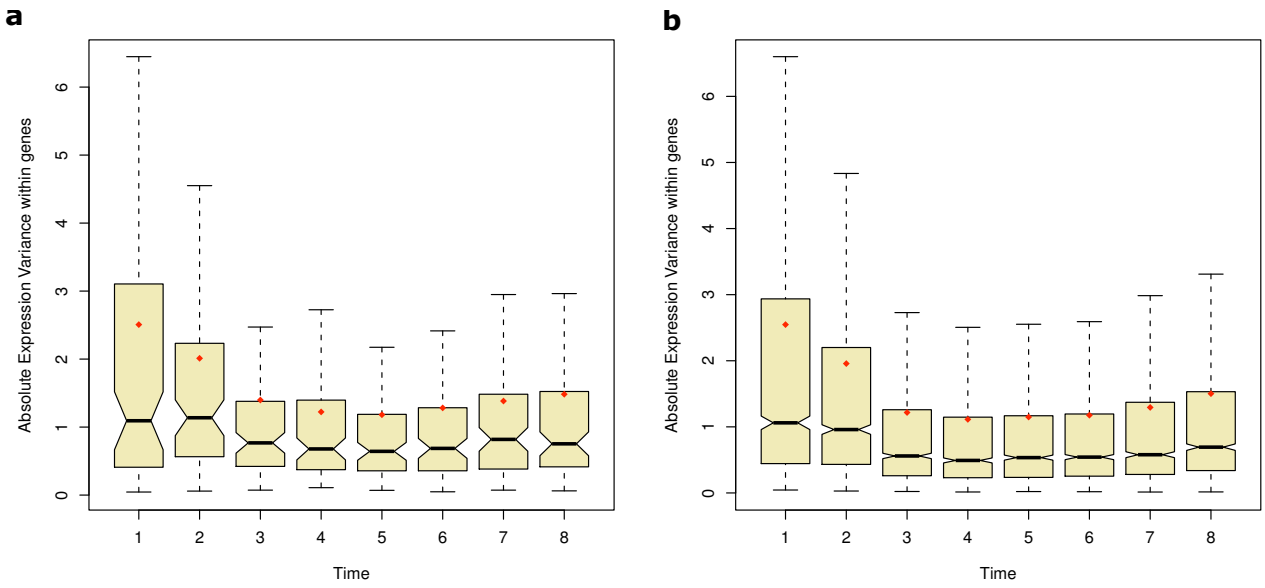

Supplementary Figure 8. Within-gene variance in absolute log_2 expression levels as a function of time. **a**, The top 100 genes that correlate positively with the hourglass pattern of temporal divergence. **b**, 1188 genes that each fit their variance in absolute expression levels to second order polynomials with minima that fall within the time-course. Functional analyses of these genes shows that they are involved in developmental processes (Supplementary Tables 4, 5, and 6) and they have a significantly higher mean correlation with the global hourglass temporal divergence profile than the mean across all genes in the dataset (Supplementary Information). Red diamonds indicate the mean.

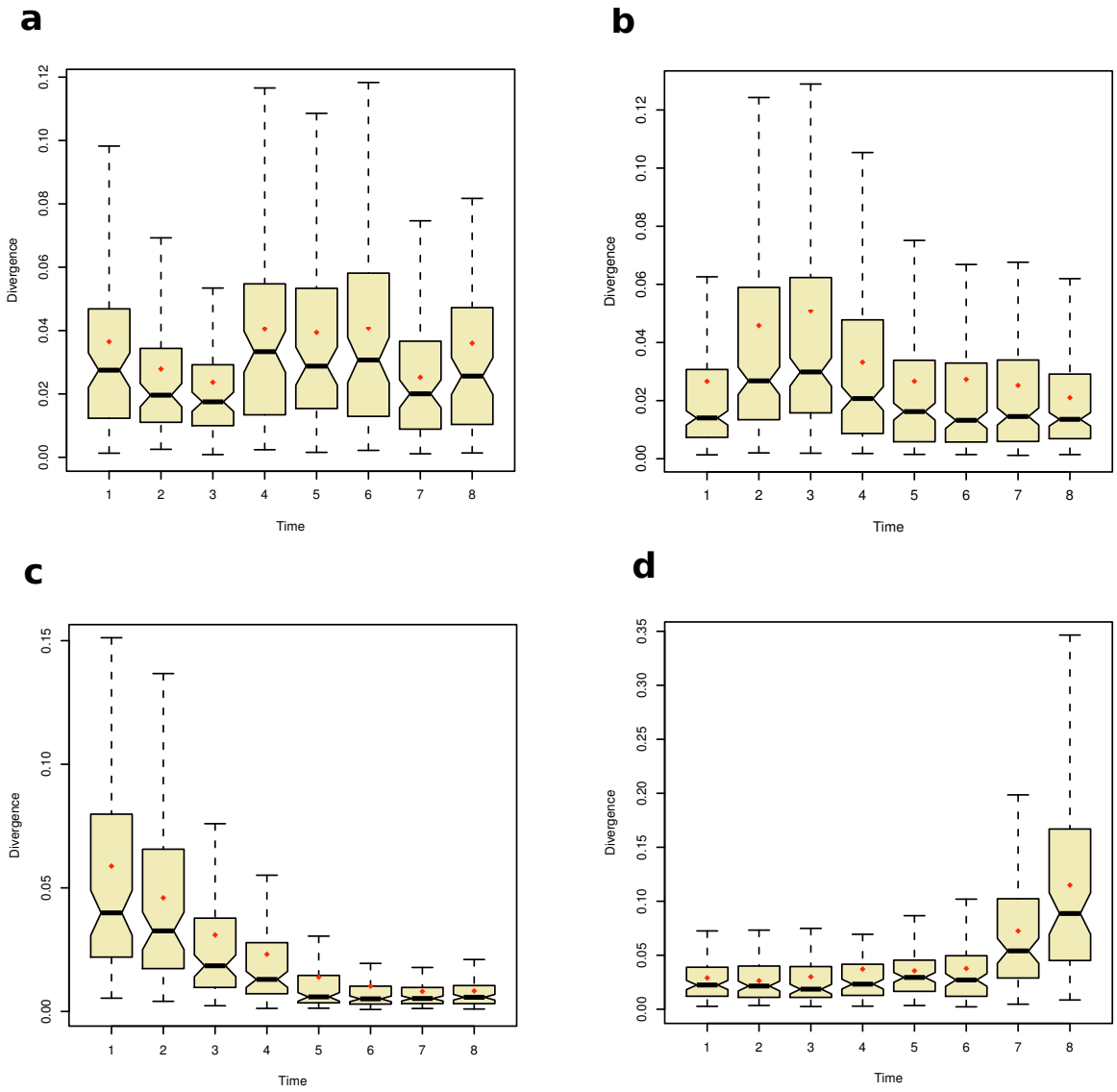

Supplementary Figure 9. Sets of genes that deviate from the hourglass temporal divergence profile. **a**, The top 100 genes that correlate positively with a profile where divergence peaks at time points 4, 5, and 6. By correlating each gene's divergence profile with a profile where divergence peaks during mid-embryogenesis, we ranked genes according to their tendency to deviate from the hourglass pattern. **b**, 200 genes whose divergence profiles fit a negative quadratic coefficient to a second order polynomial. **c**, The top 100 genes that correlate positively with a linearly decreasing divergence profile. **d**, The top 100 genes that correlate positively with a linearly increasing divergence profile. Red diamonds indicate the mean.

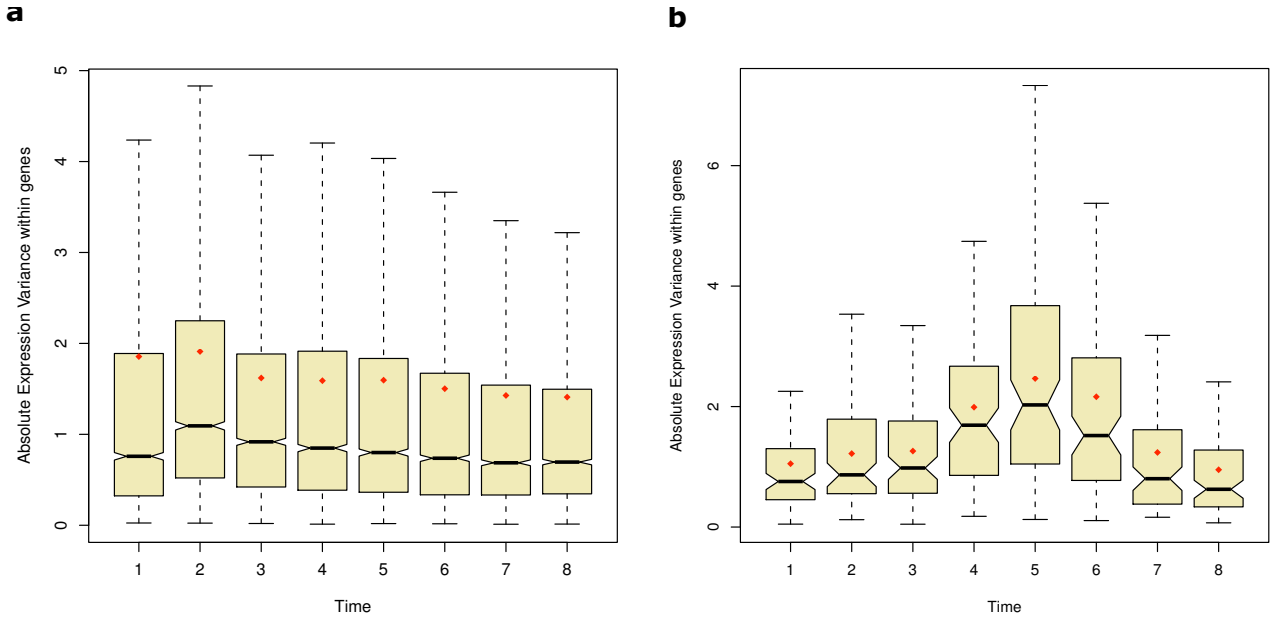

Supplementary Figure 10. Within-gene variance in absolute log_2 expression levels for **a**, all genes in the dataset, and **b**, the top 100 genes that correlate positively with a temporal divergence profile with maximal divergence during mid-embryogenesis (Supplemetary Fig. 9a). Red diamonds indicate the mean.

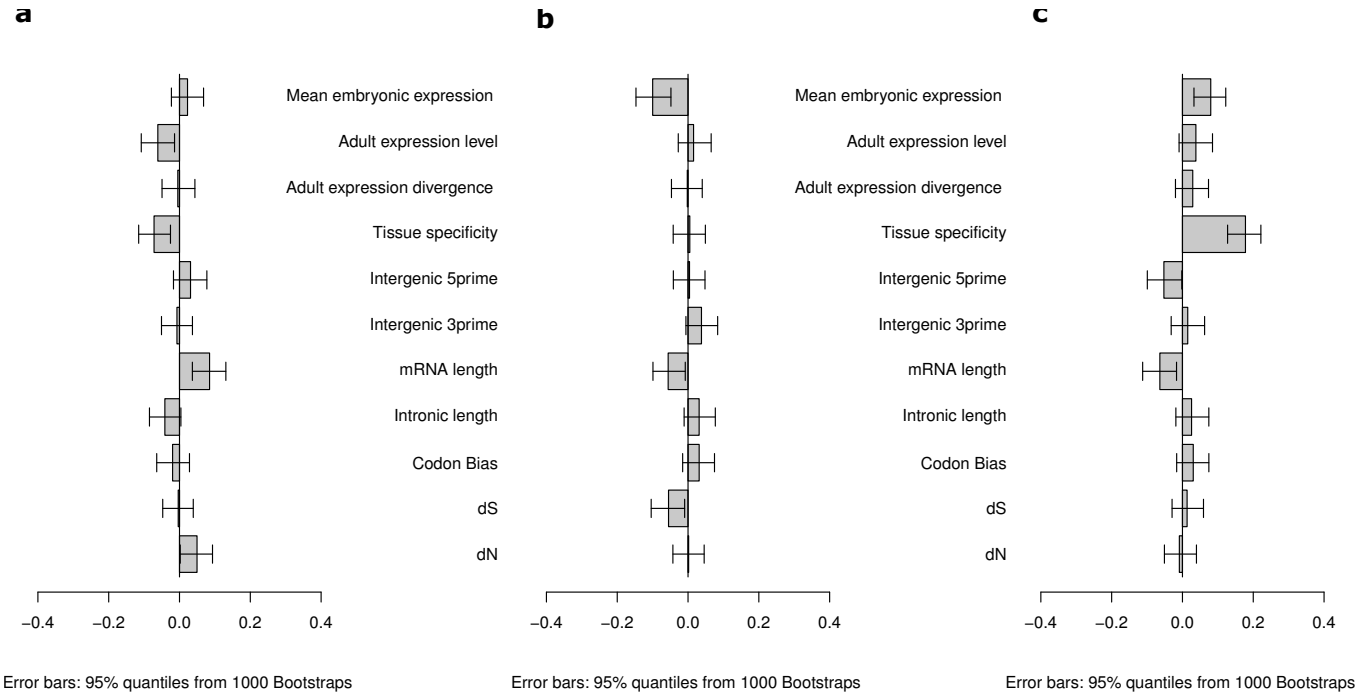

Supplementary Figure 11. **a**, Gene-level correlates for genes that correlate positively with the global hourglass profile showing a tendency for weak adult expression, broad expression patterns, and long proteins.**b**, Gene level correlates for genes that tend to diverge most at time points 4, 5, and 6 (Supplementary Fig. 9a). **c**, Gene level correlates for genes that tend to correlate positively with a linearly increasing divergence profile (Supplementary Fig. 9d).

Supplementary Tables

Supplementary Table 1. Characterisation of genes driving the global hourglass pattern of temporal divergence using a Kolmogorov-Smirnov test.

Ontology	ID	Term	#	P-value	P_{adj}-value
BP	GO:0044260	cellular macromolecule metabolic process	686	1.6×10^{-9}	2.9×10^{-6}
	GO:0010467	gene expression	441	9.6×10^{-7}	1.0×10^{-3}
	GO:0003002	regionalization	114	5.8×10^{-6}	3.7×10^{-3}
	GO:0048731	system development	386	1.4×10^{-5}	4.3×10^{-3}
	GO:0045165	cell fate commitment	76	1.6×10^{-5}	4.3×10^{-3}
	GO:0007389	pattern specification process	121	1.9×10^{-5}	4.3×10^{-3}
	GO:0048513	organ development	311	1.9×10^{-5}	4.3×10^{-3}
	GO:0048856	anatomical structure development	444	7.6×10^{-5}	1.1×10^{-2}
	GO:0007399	nervous system development	191	2.9×10^{-4}	3.0×10^{-2}
MF	GO:0003676	nucleic acid binding	415	3.6×10^{-6}	5.4×10^{-3}
CC	GO:0005622	intracellular	1161	4.9×10^{-6}	2.8×10^{-3}

Enrichment is based on the Kolmogorov-Smirnov test applied to genes ranked by their correlation to the global hourglass temporal divergence profile. BP - biological process, MF - molecular function, CC - cellular component, # - total number of genes with this annotation in the dataset. P_{adj}-value - adjusted according to the Benjamini-Hochberg false discovery rate.

Supplementary Table 2. Characterisation of genes driving the global hourglass pattern of temporal divergence taking into account local dependencies between terms in the GO hierarchy.

Ontology	ID	Term	#	*P*-value
BP	GO:0034960	cellular biopolymer metabolic process	685	1.9×10^{-4}
	GO:0010160	formation of organ boundary	7	8.8×10^{-4}
	GO:0001709	cell fate determination	42	1.0×10^{-3}
	GO:0048749	compound eye development	73	1.3×10^{-3}
	GO:0006355	regulation of transcription	164	1.9×10^{-3}
	GO:0007431	salivary gland development	57	3.4×10^{-3}
	GO:0048867	stem cell fate determination	13	3.6×10^{-3}
	GO:0010467	gene expression	441	3.8×10^{-3}
	GO:0007409	axonogenesis	51	4.2×10^{-3}
	GO:0007417	central nervous system development	52	5.2×10^{-3}
	GO:0051093	negative regulation of developmental process	33	8.7×10^{-3}
MF	GO:0003700	transcription factor activity	117	2.9×10^{-4}
	GO:0003676	nucleic acid binding	415	6.0×10^{-4}
CC	GO:0005634	nucleus	449	9.3×10^{-4}
	GO:0044424	intracellular part	1054	4.8×10^{-3}

Enrichment is based on the 'elim' algorithm in the topGO R package and the Kolmogorov-Smirnov test applied to genes ranked by their correlation to the global hourglass temporal divergence profile. BP - biological process, MF - molecular function, CC - cellular component, # - total number of genes with this annotation in the dataset.

Supplementary Table 3. Characterisation of genes driving the global hourglass pattern of temporal divergence taking into account the inheritance bias for parent-child relationships.

Ontology	ID	Term	#	Significant	Expected	*P*-value
BP	GO:0001709	cell fate determination	42	27	13.91	7.4×10^{-5}
	GO:0035152	regulation of tube architecture	14	10	4.64	8.0×10^{-5}
	GO:0022612	gland morphogenesis	51	26	16.89	7.9×10^{-3}
	GO:0032502	developmental process	542	202	179.47	9.3×10^{-3}
	GO:0048513	organ development	311	126	102.98	1.0×10^{-2}
	GO:0014016	neuroblast differentiation	10	8	3.31	1.0×10^{-2}
	GO:0048598	embryonic morphogenesis	63	31	20.86	1.3×10^{-2}
MF	GO:0003676	nucleic acid binding	415	157	136.34	5.9×10^{-3}
CC	GO:0005634	nucleus	449	164	149.48	7.2×10^{-3}

Enrichment is based on the 'parent-child' algorithm in the topGO R package and Fisher's exact test applied to the top 1000 genes positively correlated to the global hourglass temporal divergence profile. BP - biological process, MF - molecular function, CC - cellular component, # - total number of genes with this annotation in the dataset.

Supplementary Table 4. Characterisation of 1188 genes that follow an hourglass divergence pattern both in terms of temporal dynamics and variance of absolute expression levels.

Ontology	ID	Term	#	Significant	Expected	P-value	P_{adj}-value
BP	GO:0048513	organ development	311	165	126.78	1.2×10^{-6}	3.6×10^{-3}
	GO:0010467	gene expression	441	220	179.78	6.8×10^{-6}	7.5×10^{-3}
	GO:0048856	anatomical structure development	444	220	181	1.3×10^{-5}	9.7×10^{-3}
	GO:0048731	system development	386	194	157.35	1.6×10^{-5}	9.7×10^{-3}
	GO:0010468	regulation of gene expression	250	132	101.91	2.6×10^{-5}	1.2×10^{-2}
	GO:0007517	muscle organ development	58	39	23.64	3.2×10^{-5}	1.2×10^{-2}
	GO:0009888	tissue development	149	84	60.74	4.6×10^{-5}	1.2×10^{-2}
	GO:0001709	cell fate determination	42	30	17.12	4.7×10^{-5}	1.2×10^{-2}
MF	GO:0003702	RNA pol II TF activity	82	51	32.67	2.6×10^{-5}	3.6×10^{-2}
CC	GO:0005634	nucleus	449	237	184.91	3.5×10^{-9}	1.9×10^{-6}

Enrichment is based on Fisher's exact test applied to 1188 genes that follow an hourglass divergence pattern both in terms of temporal dynamics and variance of absolute expression levels (Supplementary Fig. 8b and Supplementary Information). BP - biological process, MF - molecular function, CC - cellular component, TF - transcription factor, pol - polymerase, # - total number of genes with this annotation in the dataset.

Supplementary Table 5. Characterisation of 1188 genes that follow an hourglass divergence pattern both in terms of temporal dynamics and variance of absolute expression levels taking into account local dependencies between terms in the GO hierarchy.

Ontology	ID	Term	#	Significant	Expected	*P*-value
BP	GO:0007517	muscle organ development	58	39	23.64	3.2×10^{-5}
	GO:0030261	chromosome condensation	12	11	4.89	3.7×10^{-4}
	GO:0006367	transcription initiation from RNA pol	24	18	9.78	6.6×10^{-4}
	GO:0007052	mitotic spindle organization	65	39	26.5	1.1×10^{-3}
	GO:0007498	mesoderm development	32	22	13.04	1.1×10^{-3}
	GO:0035051	cardiac cell differentiation	7	7	2.85	1.8×10^{-3}
	GO:0007400	neuroblast fate determination	10	9	4.08	1.9×10^{-3}
	GO:0007409	axonogenesis	51	31	20.79	2.7×10^{-3}
	GO:0001709	cell fate determination	42	30	17.12	3.3×10^{-3}
	GO:0045449	regulation of transcription	204	108	83.16	3.8×10^{-3}
	GO:0007419	ventral cord development	14	11	5.71	4.5×10^{-3}
	GO:0007398	ectoderm development	27	18	11.01	5.5×10^{-3}
MF	GO:0003729	mRNA binding	56	34	22.31	1.1×10^{-3}
	GO:0003702	RNA pol II TF activity	82	51	32.67	1.5×10^{-3}
CC	GO:0005634	nucleus	449	237	184.91	4.6×10^{-5}

Enrichment is based on the 'elim' algorithm in the topGO R package and Fisher's exact test applied to 1188 genes that follow an hourglass divergence pattern both in terms of temporal dynamics and variance of absolute expression levels (Supplementary Fig. 8b and Supplementary Information). BP - biological process, MF - molecular function, CC - cellular component, TF - transcription factor, pol - polymerase, # - total number of genes with this annotation in the dataset.

Supplementary Table 6. Characterisation of 1188 genes that follow an hourglass divergence pattern both in terms of temporal dynamics and variance of absolute expression levels taking into account inheritance bias for parent-child relationships.

Ontology	ID	Term	#	Significant	Expected	*P*-value
BP	GO:0080090	regulation of primary metabolic process	274	139	111.7	1.1×10^{-4}
	GO:0006323	DNA packaging	17	15	6.93	1.7×10^{-4}
	GO:0010467	gene expression	441	220	179.78	1.9×10^{-4}
	GO:0051674	localization of cell	82	49	33.43	2.1×10^{-3}
	GO:0032502	developmental process	542	254	220.95	4.3×10^{-3}
	GO:0048869	cellular developmental process	293	147	119.44	5.0×10^{-3}
	GO:0048856	anatomical structure development	444	220	181	5.0×10^{-3}
MF	GO:0030528	transcription regulator activity	204	105	81.29	2.8×10^{-4}
CC	GO:0005634	nucleus	449	237	184.91	8.7×10^{-8}

Enrichment is based on the 'parent-child' algorithm in the topGO R package and Fisher's exact test applied to 1188 genes that follow an hourglass divergence pattern both in terms of temporal dynamics and variance of absolute expression levels (Supplementary Fig. 8b and Supplementary Information). BP - biological process, MF - molecular function, CC - cellular component, TF - transcription factor, pol - polymerase, # - total number of genes with this annotation in the dataset.

Supplementary Table 7. Characterisation of genes that don't follow an hourglass pattern of temporal divergence.

Ontology	ID	Term	#	*P*-value
BP	GO:0006979	response to oxidative stress	15	5.5×10^{-4}
	GO:0006727	ommochrome biosynthetic process	8	2.3×10^{-3}
	GO:0045087	innate immune response	17	3.1×10^{-3}
	GO:0042060	wound healing	8	9.5×10^{-3}
	GO:0006030	chitin metabolic process	22	1.2×10^{-2}
	GO:0009611	response to wounding	8	2.3×10^{-2}
	GO:0019731	antibacterial humoral response	8	2.8×10^{-2}
CV	267	yolk nuclei (stage 2)	245	2.3×10^{-8}
	472	yolk nuclei (stage 3)	232	1.2×10^{-6}
	474	yolk nuclei (stage 5)	200	2.8×10^{-6}
	473	yolk nuclei (stage 4)	220	7.0×10^{-6}
	472	no staining (stage 1)	232	1.6×10^{-5}
	115	embryonic/larval fat body (stage 6)	208	6.3×10^{-4}
	203	procrystal cell (stage 5)	84	2.9×10^{-3}

Enrichment is based on the 'elim' algorithm in the topGO R package and the Kolmogorov-Smirnov test applied to genes that don't follow an hourglass divergence pattern. BP - biological process, CV - controlled vocabulary, # - total number of genes with this annotation in the dataset. Stages from ref [**?**].

Supplementary Table 8. Enriched GO terms for quantitative divergence (variance in GS values).

	Ontology	ID	Term	#	*P*-value
Conserved	BP	GO:0006412	translation	112	3.3×10^{-5}
		GO:0006396	RNA processing	90	5.6×10^{-4}
		GO:0045449	regulation of transcription	204	1.1×10^{-3}
		GO:0050794	regulation of cellular process	574	2.4×10^{-3}
	MF	GO:0003735	structural constituent of ribosome	58	2.7×10^{-5}
		GO:0005524	ATP binding	205	4.3×10^{-4}
		GO:0030528	transcription regulator activity	204	5.9×10^{-4}
	CC	GO:0044428	nuclear part	172	1.0×10^{-4}
		GO:0022625	cytosolic large ribosomal subunit	9	1.2×10^{-3}
		GO:0043231	intracellular membrane-bounded organelle	742	4.1×10^{-3}
Divergent	BP	GO:0006030	chitin metabolic process	22	1.2×10^{-4}
		GO:0006979	response to oxidative stress	15	1.1×10^{-3}
		GO:0006635	fatty acid beta-oxidation	7	1.6×10^{-3}
		GO:0046164	alcohol catabolic process	15	9.8×10^{-3}
		GO:0005996	monosaccharide metabolic process	51	1.0×10^{-2}
	MF	GO:0008061	chitin binding	17	8.8×10^{-4}
		GO:0003995	acyl-CoA dehydrogenase activity	6	1.8×10^{-3}
		GO:0004601	peroxidase activity	10	2.0×10^{-3}
		GO:0070011	peptidase activity, acting on L-amino acids	114	8.4×10^{-3}
	CC	GO:0005792	microsome	17	4.7×10^{-3}
		GO:0005764	lysosome	7	5.0×10^{-3}
		GO:0005576	extracellular region	89	2.1×10^{-2}

Enrichment is based on the 'elim' algorithm in the topGO R package and the Kolmogorov-Smirnov test applied to genes ranked by variance in GS values. BP - biological process, MF - molecular function, CC - cellular component, # - total number of genes with this annotation in the dataset.

Supplementary Table 9. Enriched GO terms for temporal divergence at time point 1.

	Ontology	ID	Term	#	*P*-value
Conserved	BP	GO:0006412	translation	122	2.5×10^{-7}
		GO:0006120	mitochondrial electron transport, NADH to ubiquinone	11	4.8×10^{-6}
		GO:0000398	nuclear mRNA splicing, via spliceosome	42	1.4×10^{-5}
		GO:0000022	mitotic spindle elongation	25	1.9×10^{-5}
		GO:0006886	intracellular protein transport	58	1.7×10^{-4}
	MF	GO:0003735	structural constituent of ribosome	58	1.9×10^{-10}
		GO:0003729	mRNA binding	56	9.5×10^{-8}
		GO:0005524	ATP binding	205	1.8×10^{-4}
	CC	GO:0005681	spliceosomal complex	17	1.1×10^{-6}
		GO:0043234	protein complex	329	1.3×10^{-6}
		GO:0044455	mitochondrial membrane part	33	1.1×10^{-4}
		GO:0005622	intracellular	1161	1.5×10^{-4}
Divergent	BP	GO:0007498	mesoderm development	32	2.5×10^{-5}
		GO:0006030	chitin metabolic process	22	8.1×10^{-4}
		GO:0007354	zygotic determination of anterior/posterior axis	13	1.3×10^{-3}
		GO:0006520	cellular amino acid metabolic process	64	7.1×10^{-3}
		GO:0007313	maternal specification of dorsal/ventral axis	4	1.0×10^{-2}
	MF	GO:0004497	monooxygenase activity	27	2.2×10^{-6}
		GO:0020037	heme binding	30	5.3×10^{-6}
		GO:0008237	metallopeptidase activity	39	1.2×10^{-5}
		GO:0003700	transcription factor activity	117	2.1×10^{-4}
		GO:0003824	catalytic activity	1064	8.3×10^{-4}
	CC	GO:0005576	extracellular region	89	7.7×10^{-7}
		GO:0005792	microsome	17	2.1×10^{-5}
		GO:0005764	lysosome	7	1.3×10^{-4}
		GO:0005887	integral to plasma membrane	42	1.9×10^{-4}

Enrichment is based on the 'elim' algorithm in the topGO R package and the Kolmogorov-Smirnov test applied to genes ranked by variance in GST values at time point 1. BP - biological process, MF - molecular function, CC - cellular component, # - total number of genes with this annotation in the dataset.

Supplementary Table 10. Enriched GO terms for temporal divergence at time point 5.

	Ontology	ID	Term	#	*P*-value
Conserved	BP	GO:0006412	translation	112	1.7×10^{-15}
		GO:0007052	mitotic spindle organization	65	5.9×10^{-6}
		GO:0006367	transcription initiation from RNA pol II prom	24	2.9×10^{-5}
		GO:0000398	nuclear mRNA splicing, via spliceosome	42	1.6×10^{-4}
		GO:0007049	cell cycle	167	3.8×10^{-4}
	MF	GO:0003735	structural constituent of ribosome	58	3.4×10^{-17}
		GO:0003729	mRNA binding	56	1.3×10^{-7}
		GO:0003676	nucleic acid binding	415	5.4×10^{-7}
	CC	GO:0005622	intracellular	1161	2.4×10^{-9}
		GO:0043234	protein complex	329	2.6×10^{-7}
		GO:0044428	nuclear part	172	8.3×10^{-5}
Divergent	BP	GO:0006030	chitin metabolic process	22	1.9×10^{-7}
		GO:0005975	carbohydrate metabolic process	113	9.4×10^{-5}
		GO:0006508	proteolysis	136	2.2×10^{-4}
		GO:0006952	defense response	43	3.7×10^{-4}
	MF	GO:0004497	monooxygenase activity	27	4.0×10^{-9}
		GO:0020037	heme binding	30	8.4×10^{-8}
		GO:0008061	chitin binding	17	1.2×10^{-7}
	CC	GO:0005576	extracellular region	89	3.0×10^{-12}
		GO:0005792	microsome	17	2.4×10^{-7}
		GO:0016021	integral to membrane	195	4.2×10^{-5}

Enrichment is based on the 'elim' algorithm in the topGO R package and the Kolmogorov-Smirnov test applied to genes ranked by variance in GST values at time point 5. BP - biological process, MF - molecular function, CC - cellular component, # - total number of genes with this annotation in the dataset, pol - polymerase, prom - promoter.

Supplementary Table 11. Enriched GO terms for temporal divergence at time point 8.

	Ontology	ID	Term	#	*P*-value
Conserved	BP	GO:0006412	translation	112	1.9×10^{-7}
		GO:0009987	cellular process	1488	3.7×10^{-6}
		GO:0000022	mitotic spindle elongation	25	5.3×10^{-6}
		GO:0006886	intracellular protein transport	58	1.7×10^{-5}
	MF	GO:0003735	structural constituent of ribosome	58	9.1×10^{-9}
		GO:0003729	mRNA binding	56	4.4×10^{-7}
		GO:0005515	protein binding	458	1.0×10^{-5}
	CC	GO:0005622	intracellular	1161	1.7×10^{-8}
		GO:0005634	nucleus	449	3.6×10^{-8}
		GO:0030529	ribonucleoprotein complex	101	2.7×10^{-5}
Divergent	BP	GO:0006030	chitin metabolic process	22	5.3×10^{-11}
		GO:0006508	proteolysis	136	3.8×10^{-7}
		GO:0046700	heterocycle catabolic process	7	4.3×10^{-4}
		GO:0006952	defense response	43	6.0×10^{-4}
	MF	GO:0008061	chitin binding	17	9.8×10^{-11}
		GO:0004497	monooxygenase activity	27	2.2×10^{-10}
		GO:0020037	heme binding	25	1.5×10^{-8}
	CC	GO:0005576	extracellular region	89	2.1×10^{-10}
		GO:0005792	microsome	17	1.7×10^{-7}
		GO:0016021	integral to membrane	195	5.6×10^{-5}

Enrichment is based on the 'elim' algorithm in the topGO R package and the Kolmogorov-Smirnov test applied to genes ranked by variance in GST values at time point 8. BP - biological process, MF - molecular function, CC - cellular component, # - total number of genes with this annotation in the dataset.

Supplementary Information

Contents

1 Supplementary Methods

1.1 Probe selection

The aligned transcript sequences of all species were scanned with a 60 nucleotide long window (Supplementary Fig. 1). For each nucleotide position N within each window we calculated the information entropy $H(N)$ across all species. We first computed the relative frequencies $p(n)$ of all possible nucleotides $n = \{A, T, C, G, gap\}$ at a given position N in the alignment. The value *gap* was assigned to true gaps in the alignment as well as to nucleotides for which sequencing information was missing. In order to normalise the information entropy of nucleotide position $H(N)$ we divided it by H_{max}, which is the maximum possible information entropy calculated for a nucleotide position N across six species with five possible values $n = \{A, T, C, G, gap\}$,

$$H(N) = \frac{-\sum_{n=\{A,T,C,G,gap\}} p(n) log_2 p(n)}{H_{max}}.$$

The information entropy of the 60 nucleotide long candidate probe H_{60-mer} was defined as the average information entropy $H(N)$ of all nucleotide positions N in this candidate probe.

$$H_{60-mer} = \frac{\sum_{i=1}^{60} H(N)_i}{60}.$$

To reject probes situated in regions with low quality sequencing data, we counted the number of nucleotides for which sequencing information was missing. If this number exceeded 10 in two species the candidate probe was assigned the highest possible normalised entropy value of 1.

1.2 Probe orthology assignment

After aligning our chosen probes, we noticed that several of them were not hitting their correct orthologues. Therefore, we systematically identified problematic probes. Probe sequences were aligned to the genome for each respective *Drosophila* species using the Novoalign (http://www.novocraft.com/) short read aligner. Genome sequences and gene annotations were downloaded from FlyBase [53] (melanogaster v5.20, ananassae v1.3, persimilis v1.3, pseudoobscura v2.3, simulans v1.3, virilis v1.2.). A maximum of 6 mismatches in combination with single nucleotide indels were permitted; probes failing to meet this cutoff were discarded. Genes were retained for further analysis if all of the probes for that gene fell within 3kb downstream of the annotated gene end. This was required to be true for probe sets across all 6 *Drosophila* species. This was done to ensure that the genes being analyzed contained the same amount

of information for all of the species. In the few cases where a set of all probes for a gene mapped to multiple locations with equivalent spacing within a genome, they were still included for further analysis if one of those locations was within 3kb of the correct gene. This special case was permitted to account for sequences that may be duplicated across multiple scaffolds in species that are still in the early version of their genome assemblies. In the end, we retained 3019 of the 3591 genes on the arrays for further analysis.

1.3 Choice of gene-level variables

Different components of gene length may have different associations with expression divergence. Lemos et al. (2005) [26] reported a negative correlation between protein length and expression evolution (also seen in ref [49]). In addition, two previously reported relationships inspired investigation of components of non-coding gene length. Firstly, in a variety of multi-cellular organisms, broadly expressed genes (housekeeping, metabolism, ribosome, general transcription factors) are surrounded by less intergenic DNA than genes with more complex expression patterns [27, 55, 56]. Secondly, some kinds of genes with broad expression (Transcription Factor, Signal Transducer) tend to show more stable gene expression through evolutionary time than genes with more limited expression (Structural Protein, Enzyme) [30]. Hence non-coding sequence length may be expected to be positively correlated with expression evolution. To separate these conflicting patterns we separate gene length into mRNA length (sum of exons), intronic length , and the 5'- and 3'- intergenic lengths (set to zero if the gene end is nested within another gene).

2 Supplementary Results

2.1 Probe analyses

The GC content of probes shows a weak but positive relationship with expression level (Supplementary Fig. 12), and we also note a slightly reduced mean GC content for *D. virilis* probes (Supplementary Fig. 14). However, we rule out the possibility that these differences influence our measures of divergence as we see no relationship between GC content and probe overlap percentages with either quantiative or temporal measures of divergence (Supplementary Fig. 21). There is also a tendency for probes that have low GC content variation within species to show high GC content variation between species (Supplementary Fig. 15). This relationship is most likely the result of constraints resulting from our choice of probes - low GC variance within species may indicate a gene has very few places where information entropy is minimised, which in turn may indicate that the gene's nucleotide sequence is not well conserved between species,

leading to higher GC variance between species.

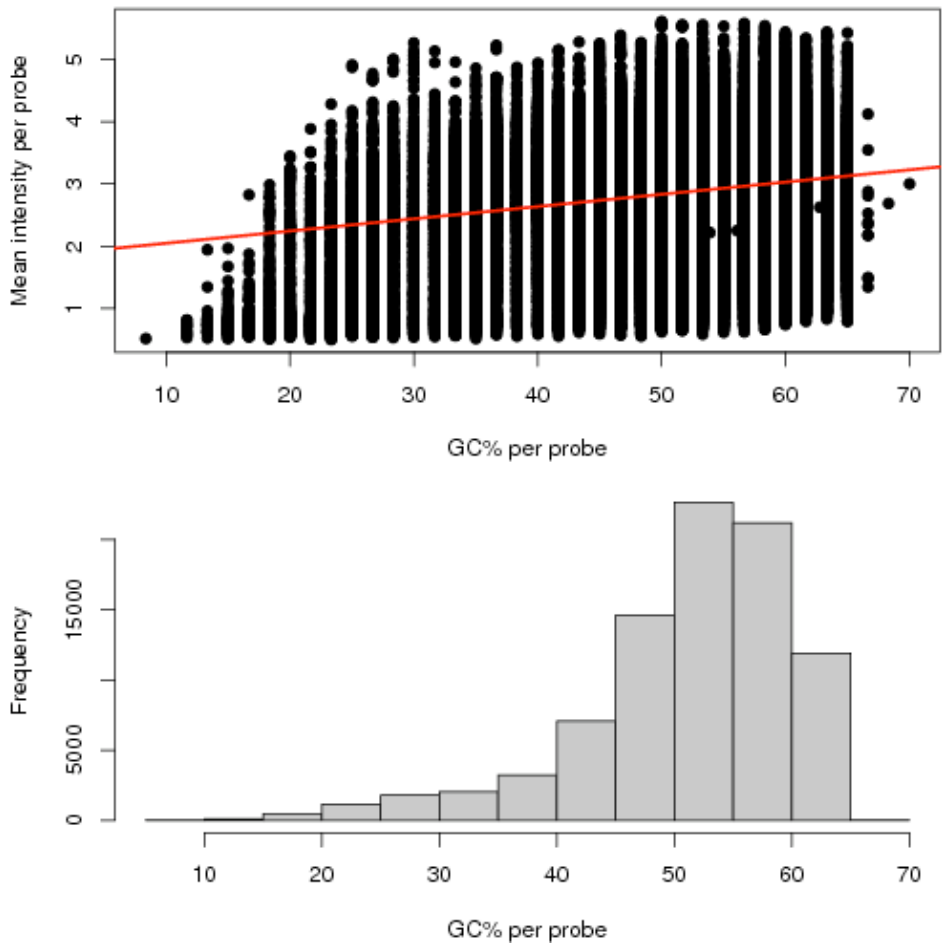

Supplementary Figure 12. The relationship between GC content of probes and their mean expression level (log_{10}), showing a weak but significantly positive relationship (top panel), and the distribution of GC percentages among all of the probes (bottom panel).

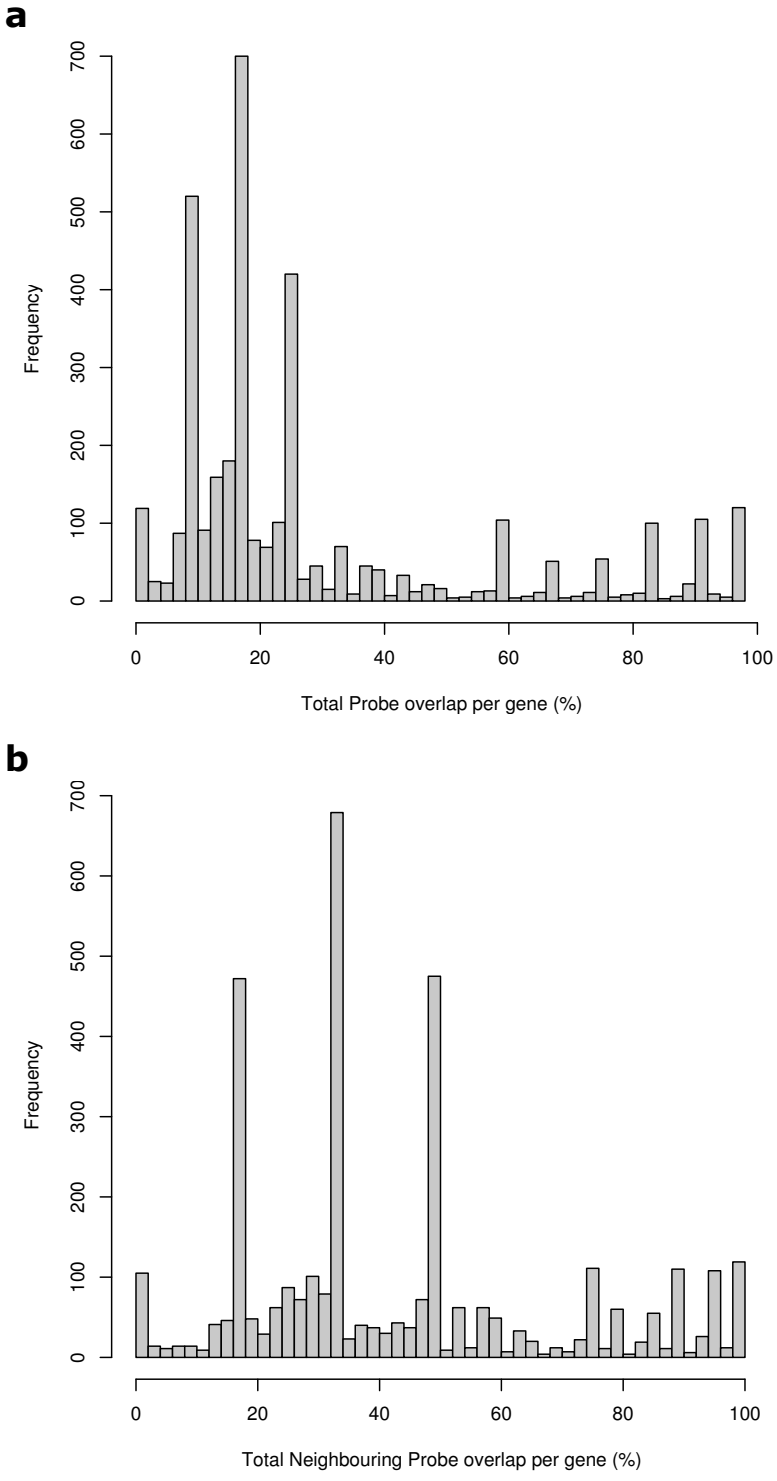

Supplementary Figure 13. **a**, The distribution of all pairwise base pair overlap percentages within each set of four probes per gene. **b**, The distribution of overlap percentages between neighbouring probes.

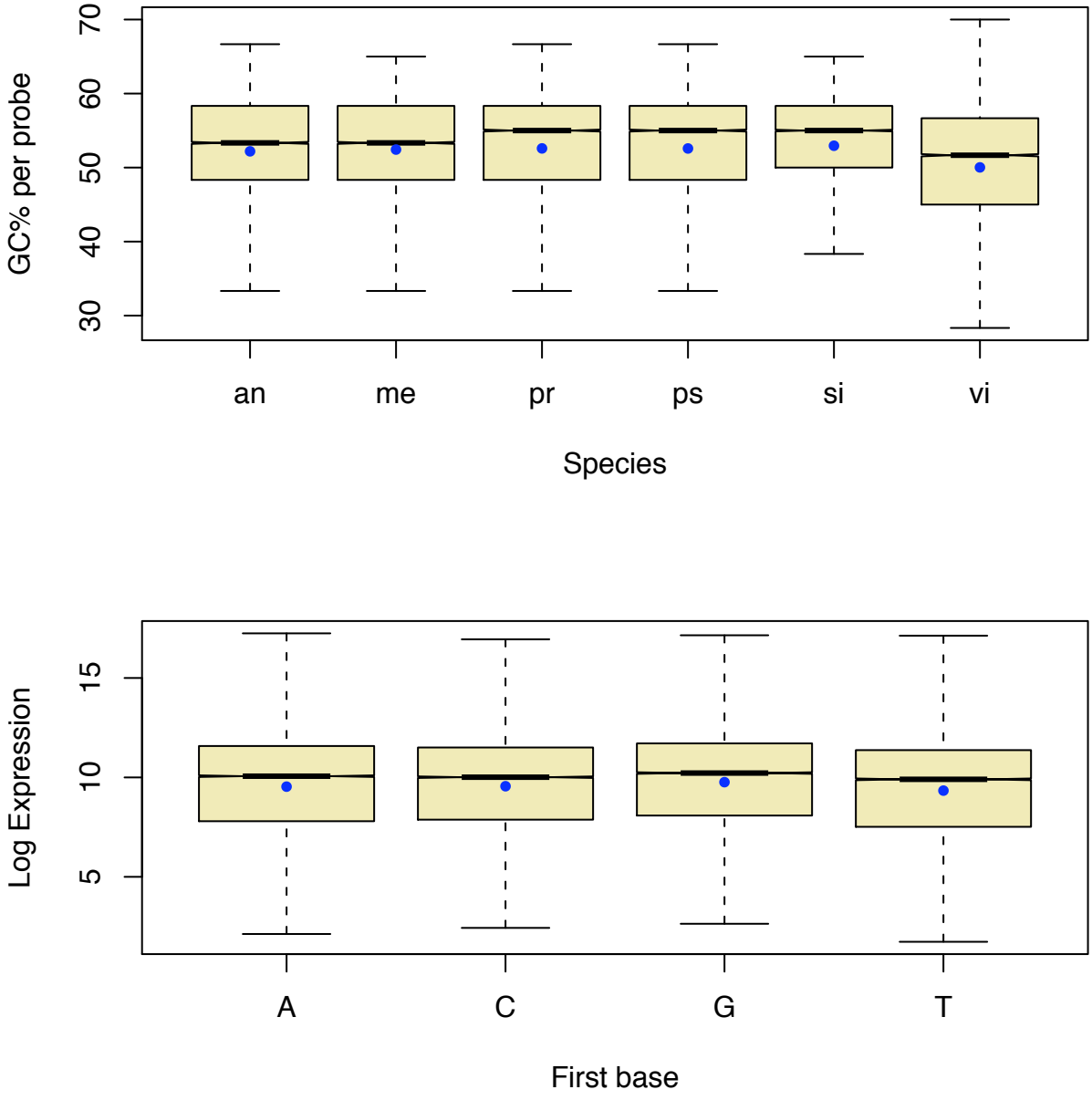

Supplementary Figure 14. Top, The distribution of GC content for probes in each species. **Bottom**, The log_2 expression level for probes with different initial bases at the 5' end. Blue circles indicate the mean.

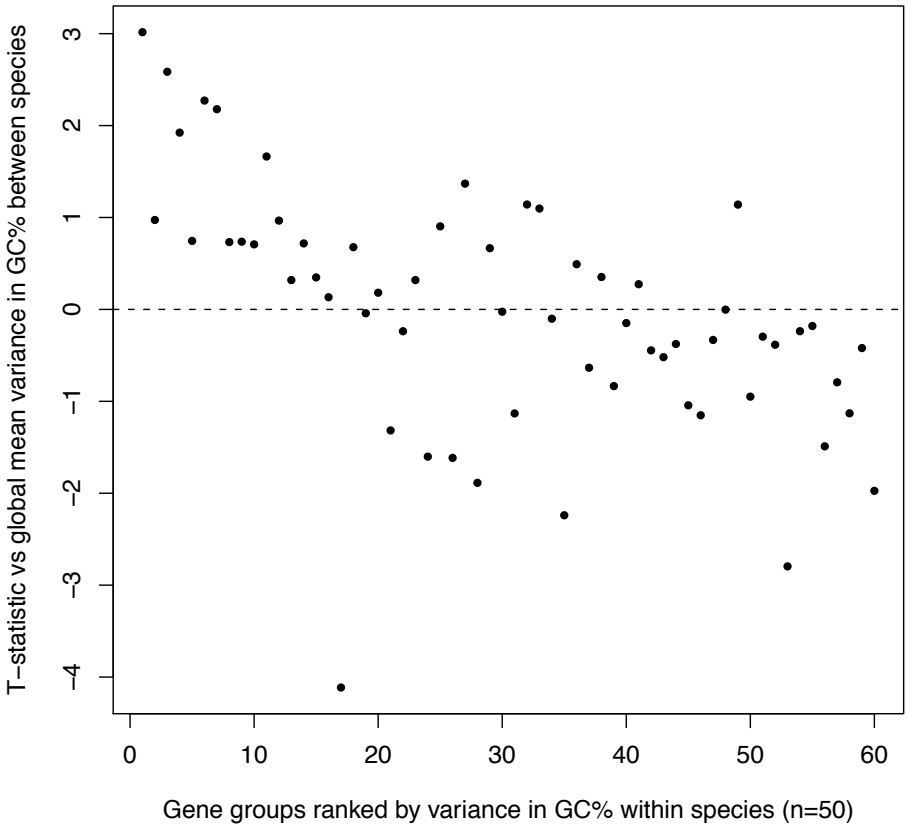

Supplementary Figure 15. The relationship between variance in GC content between probes within genes and *within* species, and the variance in GC content between probes within genes and *between* species. The relationship is visualised by ranking genes by their variance within species and grouping ranked genes into bins of 50 and computing the t-statistic against the global mean variance between species for each bin (positive values indicate a higher variance between and negative values indicate a lower variance between). The plot shows that probe sets within genes that have low variance in their GC content tend to have high variance in their GC content between species, and vice versa for probe sets with high variance in GC content within species. This negative relationship may reflect conservation at the level of nucleotide sequences between species - low variance within species may indicate the gene has very few places where information entropy is minimised, which in turn may indicate that the gene's nucleotide sequence is not well conserved between species, leading to higher variance between species.

2.2 Time-course scaling

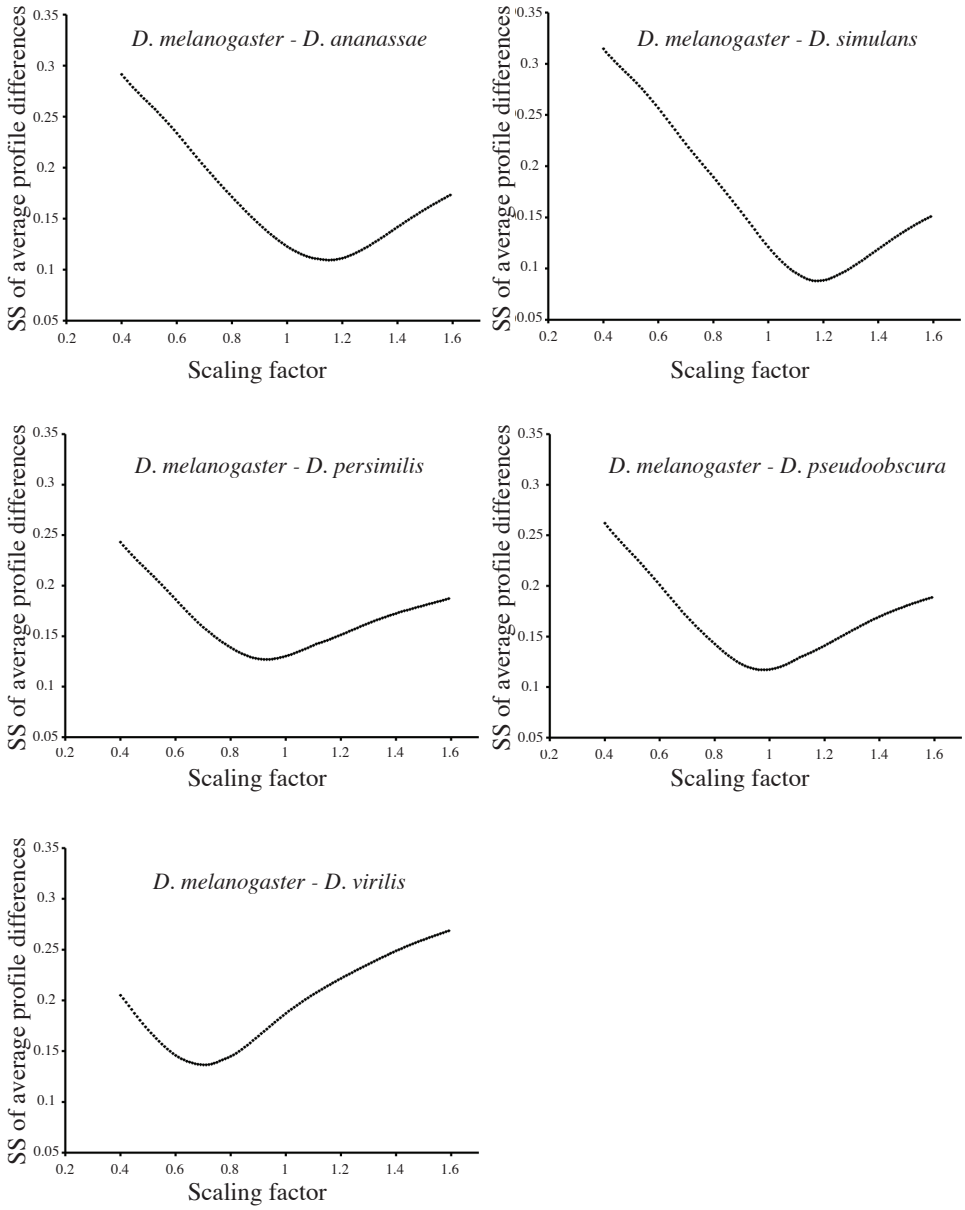

Supplementary Figure 16. Pairwise scaling graphs with *D. melanogaster* as reference. Squared sum (SS) of average differences between profiles of all (3019) genes plotted as a function of scaling factor applied.

Supplementary Table 12. Scaling factors.

Species	Scaling factor	Egg to adult developmental time (in days)
D. melanogaster	–	10
D. simulans	1.18	8
D. ananassae	1.15	8
D. persimilis	0.93	13
D. pseudoobscura	0.98	13
D. virilis	0.7	18

Scaling factors (relative to *D. melanogaster*) and egg to adult developmental time (at 25 °C) reported in [31].

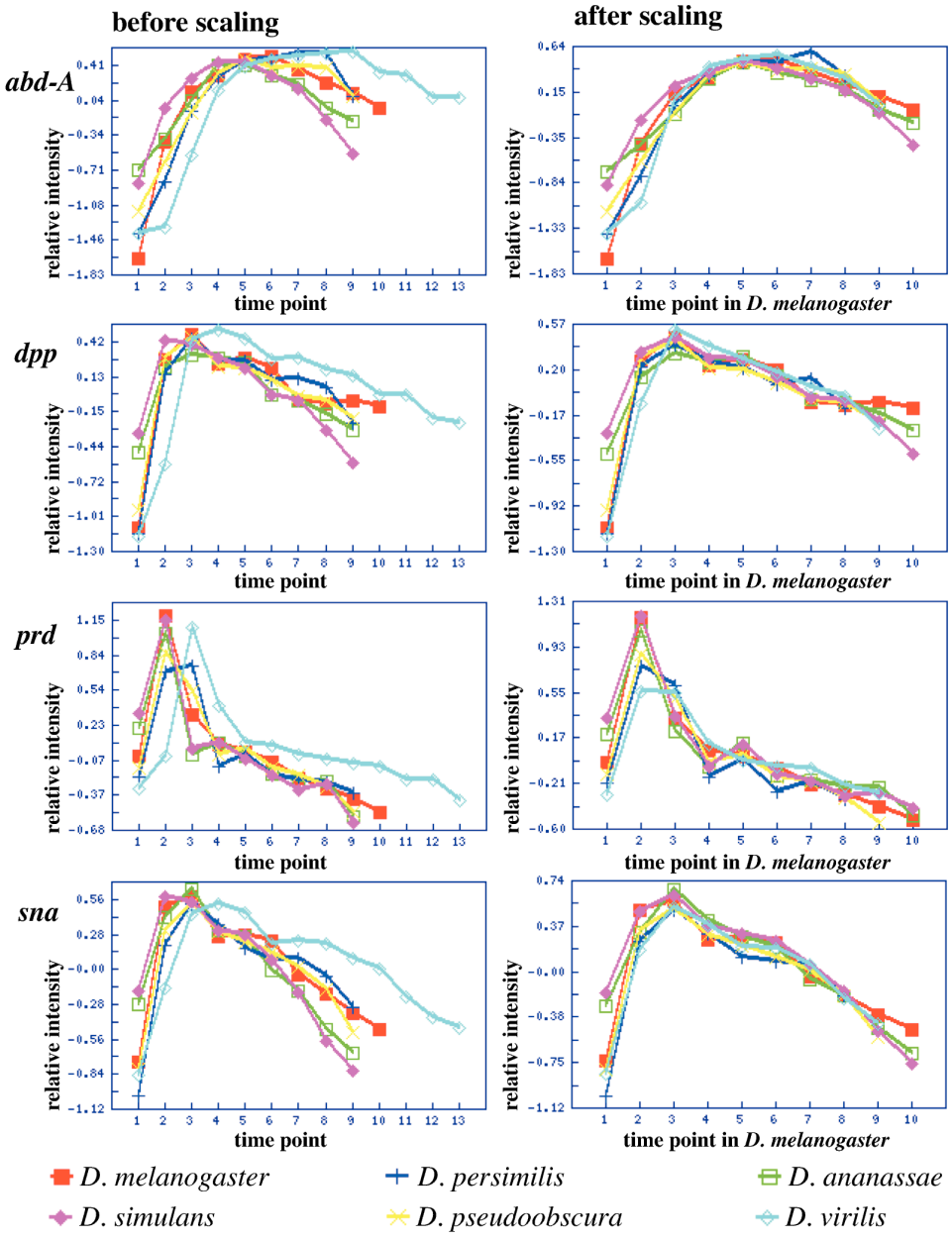

Supplementary Figure 17. Expression profiles of selected conserved developmental regulators, *abdominal A (abd-A)*, *decapentaplegic (dpp)*, *paired (prd)*, and *snail (sna)*, in six *Drosophila* species. After scaling (right column) the profiles are overlapping.

2.3 Expression dynamics

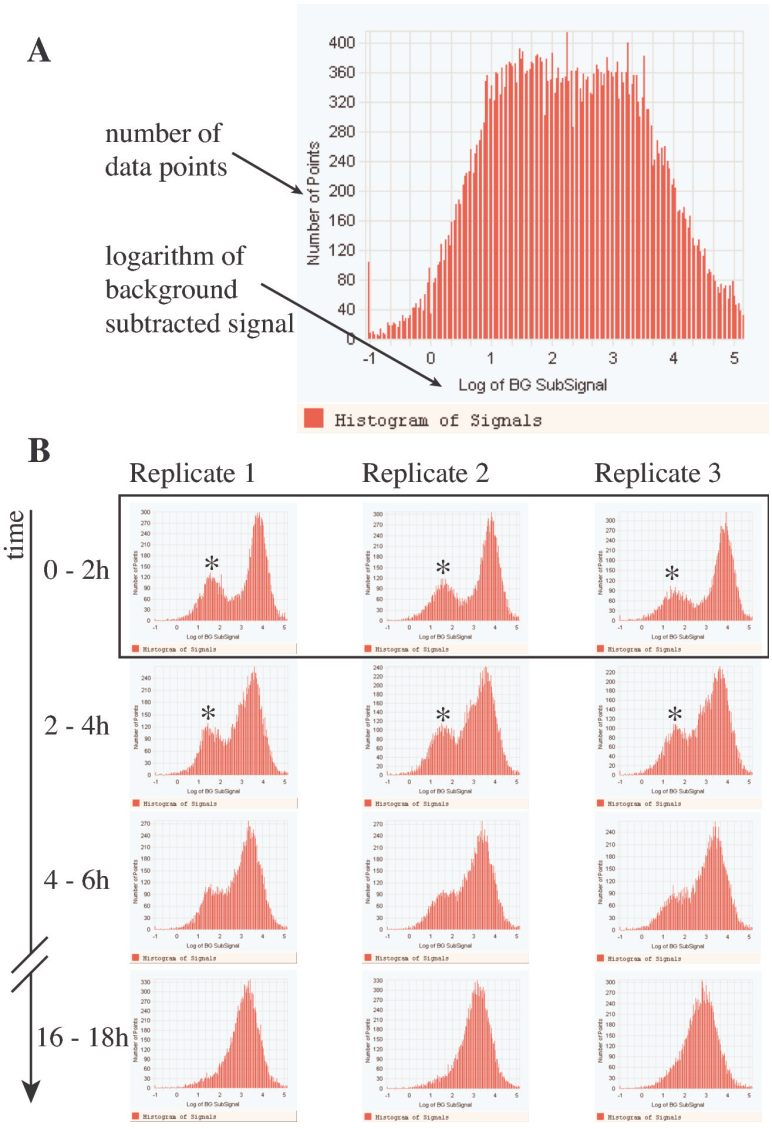

Supplementary Figure 18. **a**, Histogram of intensity signals from a human whole-genome microarray. **b**, Intensity histograms from our 'quarter-genome' microarrays. Shown is a selection of samples from three biological replicate time courses of *D. pseudoobscura* embryogenesis. The black box marks three equivalent time point data sets from all replicates that will be quantile normalized. Asterisks indicate non-specific hybridization peaks.

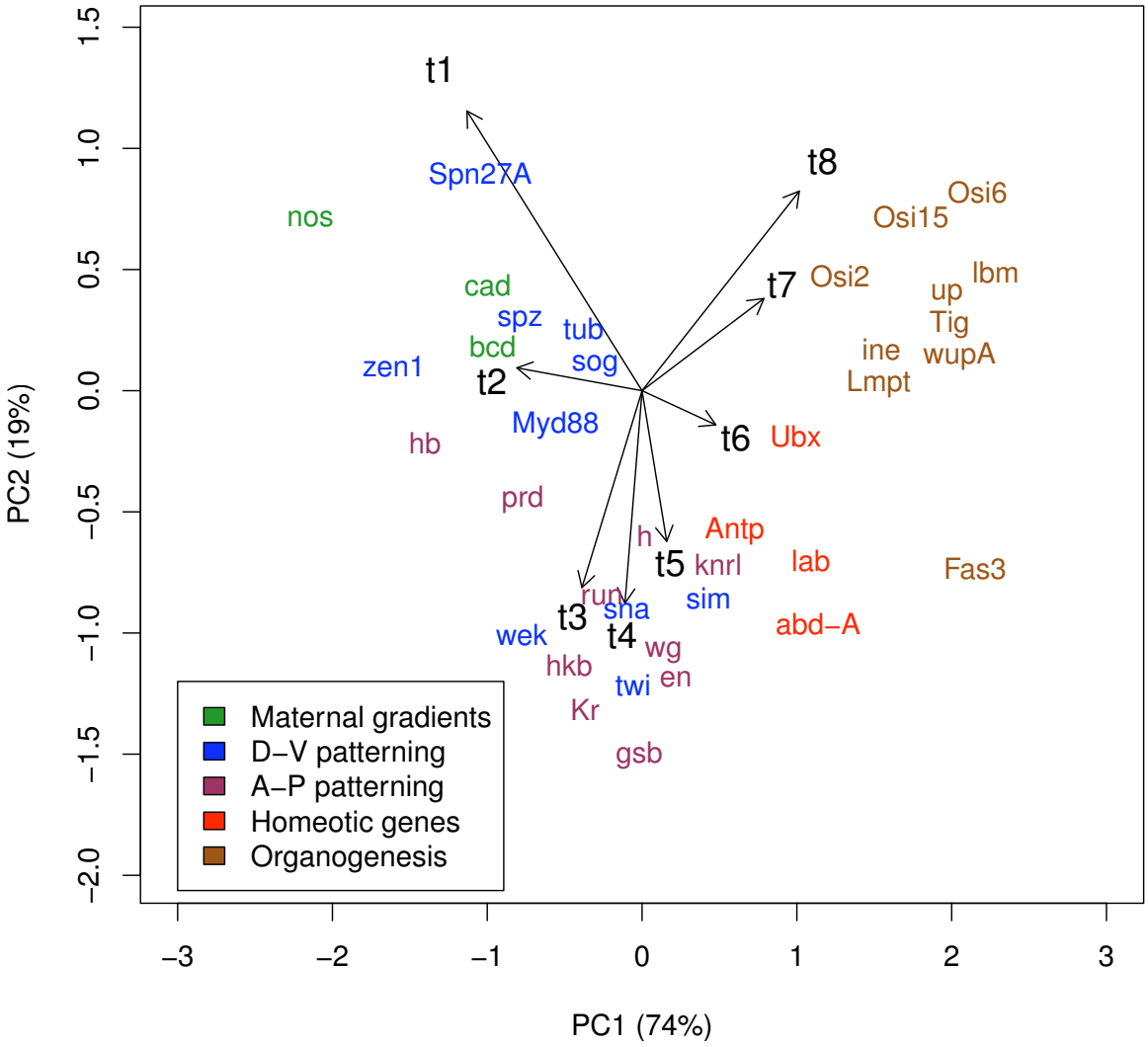

Supplementary Figure 19. The first two Principal Components for the Gene x Time (GT) effect from the global ANOVA. The position of genes on the plot shows the time at which they tend to be expressed. The plot shows that genes peak in their expression in a manner consistent with the known developmental sequence of events. D-V - Dorso-Ventral, A-P - Antero-Posterior.

2.4 ANOVA decomposition

Supplementary Table 13. ANOVA table.

Source	Degrees of Freedom	Sums of Squares	Mean Sums of Squares
Gene	3018	929956	308
Species	5	9063	1812
Time	7	6367	909
rep (Species)	12	165	13.7
probe (Gene-Species)	54342	56107	1.03
Gene x Species	15090	120550	7.99
Gene x Time	21126	183534	8.69
Species x Time	35	3285	93.8
Gene x rep (Species)	36216	4270	0.12
Time x rep (Species)	84	921	11.0
rep (Species) x probe (Gene-Species)	652104	1866	0.017
Time x probe (Gene-Species)	380394	5549	0.015
Gene x Species x Time	105630	42903	0.406
Error	431594	7889	0.018
Total	1738944	1372426	

ANOVA decomposition of log_{10} expression data. Mean sums of squares give a variance estimate for the variable in question. These variance estimates show that the fixed main factors account for the majority of the variance, and that the model accounts well for the data as shown by a small residual error variance. The interaction between time and replicates (nested in species) has a large variance for a random interaction term, but this variable is entirely confounded with array number. rep - replicates, brackets indicate nesting structure.

2.5 Random correlates of divergence

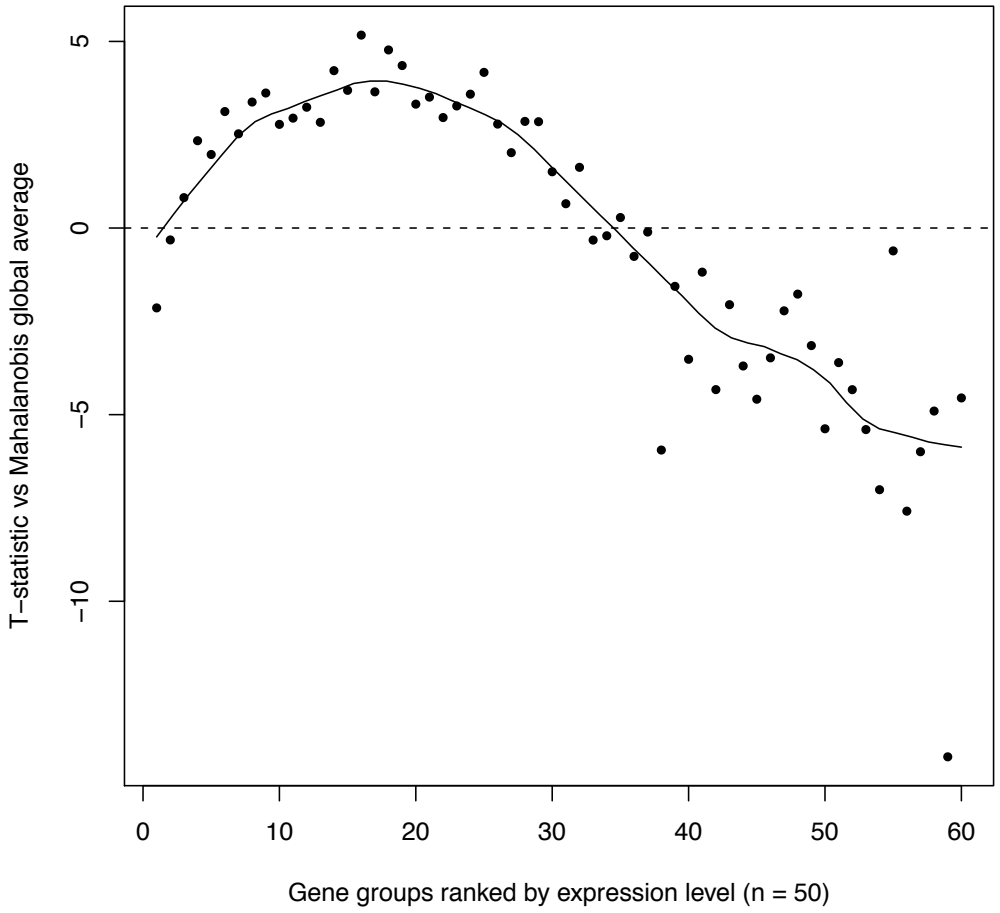

Supplementary Figure 20. The relationship between expression level and temporal divergence (Mahalanobis distance) visualised by grouping genes into bins of 50 according to mean expression level (ranked from lowest expression to highest) and for each group of 50 genes computing the t-statistic for a comparison against the global mean Mahalanobis distance (where negative values indicate the genes have on average a lower Mahalanobis distance and a positive value indicate a higher value). The plot shows that temporal divergence is not simply driven by stochastic fluctuations of very weakly expressed genes. The curve is a LOESS fit to the data.

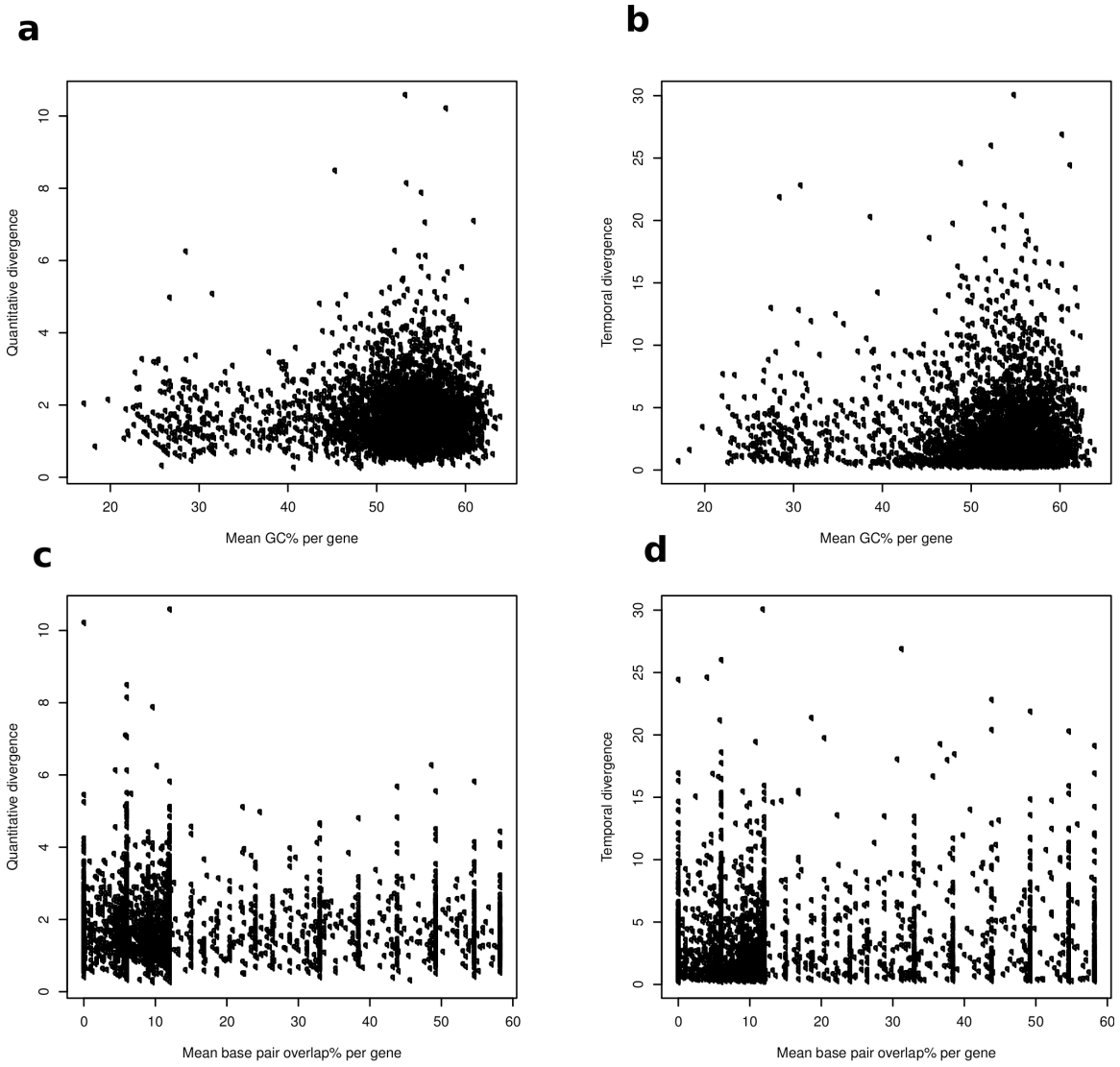

Supplementary Figure 21. The absence of relationships between probe GC content (a and b) and base pair overlap (c and d) with two measures of expression divergence: quantitative (a and c), and temporal (b and d).

2.6 Measures of divergence

Our measure of temporal divergence is the three-way interaction between genes, species, and time points, the GST values. These values capture the extent to which the temporal dynamics of different species diverge from one another at specific time points given the time-course as a whole. In this sense, GST values provide a measure of the divergence of relationships between time points thereby enabling us to identify periods in the expression profiles where a coherent flow of information from time point to time point is preserved across species. They also allow us to identify periods where there is a relative temporal disconnect between time points allowing different species to modify their expression levels in different ways. GST values achieve this by measuring the extent to which expression in a given species and time point can be explained by lower order effects, and in particular the gene-by-species (GS), and gene-by-time (GT) effects. Thus, whatever cannot be explained by average differences in expression level between species (GS effects) and average differences in expression at a particular time point (GT effect) is apportioned to the GST value.

Between-species variances in absolute expression levels within genes fail to take into account that differences in expression level at a specific time point may be partly explained by average differences in expression across time points, what we refer to as quantitative divergence (GS). However, we see that there are significant positive relationships between variances in GST values and variances in absolute expression (normalised across probes using Tukey's median polish method, and averaged over replicates) at each time point with R^2 values ranging from 0.13 to 0.34 (Supplementary Table 14). Despite this broad agreement, a high or low variance in GST values does not necessarily imply a high or low variance in absolute expression values for particular genes. To explore this relationship for genes that correlate positively with the hourglass profile, we plotted variances in absolute expression level at each time point for the top 100 genes that correlate positively with an hourglass pattern of GST divergence (Supplementary Fig. 8a). The result shows that absolute expression variances also follow the hourglass pattern for these genes, with the minimum of variance occurring in mid-embryogenesis.

To examine in more detail all of the genes that follow an hourglass shape for between-species variance in absolute expression levels we fitted second order polynomials to the variance in absolute expression levels for each gene separately and selected the genes that had minima in their curves within the time-course. In total there are 1188 genes and their variance profile also shows that expression variance is minimised during mid-embryogenesis (Supplementary Fig. 8b).

Supplementary Table 14

Time	β	P**-value**	R^2
1	18.2	$< 2 \times 10^{-16}$	0.34
2	22.8	$< 2 \times 10^{-16}$	0.25
3	23.2	$< 2 \times 10^{-16}$	0.13
4	33.4	$< 2 \times 10^{-16}$	0.15
5	43.2	$< 2 \times 10^{-16}$	0.15
6	31.9	$< 2 \times 10^{-16}$	0.14
7	21.3	$< 2 \times 10^{-16}$	0.14
8	15.9	$< 2 \times 10^{-16}$	0.13

Linear regression coefficients for absolute expression variance regressed on temporal divergence. The values show that there are significant positive relationships between variance in GST values (temporal divergence) and variance in absolute log_2 expression values at each time point.

Functional characterisation of these genes shows that they are enriched for developmental and gene expression regulation processes (Supplementary Tables 4, 5, and 6) and their mean correlation with the global hourglass temporal divergence profile is significantly higher than the mean across all of the genes (Welch's one-tailed t-test, $t = 11.69$ ($df = 2912$), $P < 2 \times 10^{-16}$). To ascertain whether weak expression early and late is driving the hourglass pattern for these genes, we compared the mean expression at each time point for these genes against the mean across all genes (Supplementary Table 15). The results show that this set of genes have significantly higher mean expression than the global mean across genes at every time point except time point 8. The increased expression is highest between time points 2 and 6.

These results show that developmental processes are enriched for hourglass patterns of divergence for both temporal divergence and divergence in absolute expression levels. Thus, there is conservation of gene expression during mid-embryogenesis both in terms of the magnitude of expression differences and in the temporal dynamics of expression, suggesting that developmental processes occurring in mid-embryogenesis are temporally connected and resistant to evolutionary change. This pattern is striking when we consider that between-species variance in absolute expression does not follow an hourglass pattern across all of the genes (Supplementary Fig. 10a), and that genes that correlate positively with divergence profiles that peak during mid-embryogenesis (Supplementary Fig. 9a) show highest variance

Supplementary Table 15

	Time							
	1	**2**	**3**	**4**	**5**	**6**	**7**	**8**
***t*-statistic**	4.17	10.0	14.5	14.2	12.6	9.14	5.12	1.50
P_{adj}**-value**	1.2 x 10^{-4}	1.8 x 10^{-15}	1.8 x 10^{-15}	1.8 x 10^{-15}	1.8 x 10^{-15}	1.8 x 10^{-15}	1.2 x 10^{-6}	0.54

Pairwise comparisons of mean expression against the global mean expression across all genes for 1188 genes that follow an hourglass pattern for both temporal divergence and absolute expression variance. The table shows that these genes tend to be more highly expressed than the average at all time points except time point 8, and that this increase is especially high between time points 2 and 6. Welch's one-tailed *t*-test, *P*-values adjusted using the Bonferroni family-wise Type I error rate.

in absolute expression during mid-embryogenesis (Supplementary Fig. 10b).

To explore whether the hourglass profile seen across genes is also reflected at the gene level we fitted second order polynomials to each gene's divergence profile and calculated the stationary point of the fitted curve. For a quadratic equation, $ax^2 + bx + c$, this is the point at which x equals $\frac{-b}{2a}$. Second differentials show that 200 genes fit maxima to their stationary points (Supplementary Fig. 9b) and these genes were discarded. An additional 104 genes have stationary points less than 1, and 237 genes have stationary points greater than 8. In total 448 genes do not have minima within the time-course and were discarded. The minima of the remaining genes cluster around time point 5 with a mean of 5.29 (Supplementary Fig 6a). There are 2421 genes with a minimum between 4 and 6.5 showing that the majority of genes have highest temporal conservation in mid-embryogenesis. This pattern shows good agreement with the number of genes that have lowest divergence at each time point (Supplementary Fig. 6b).

We also see that the majority of genes correlate positively with the global hourglass divergence profile whereas very few genes correlate positively with non-hourglass profiles or profiles that diverge late (Supplementary Fig. 7) again showing that the hourglass divergence profile is broadly represented on a gene-by-gene basis.

We carried out the same analysis for the 1188 genes that show an hourglass shape of divergence for both temporal divergence and absolute expression divergence, but this time analysing their time point minima for variance in absolute expression levels (Supplementary Fig. 22). Here we see that these genes tend to have minima in mid-embryogenesis with the mean for second order polynomials being 5.02, and

for time points for which expression variance is minimised the mean is 4.68.

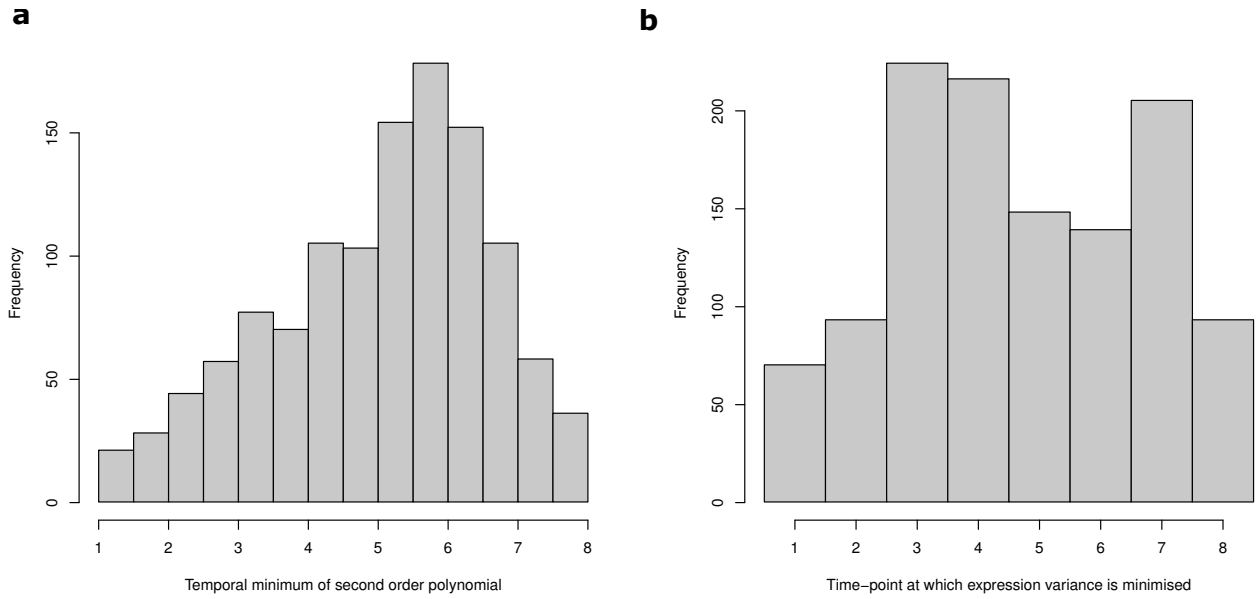

Supplementary Figure 22. The time points at which variance in absolute expression levels is minimised per gene for 1188 genes that show an hourglass shape of expression variance according to, **a**, the minima of second order polynomials fitted to each gene's variance profile, and **b**, the time point at which variance is lowest for each gene's variance profile.

2.7 Hourglass profile examples

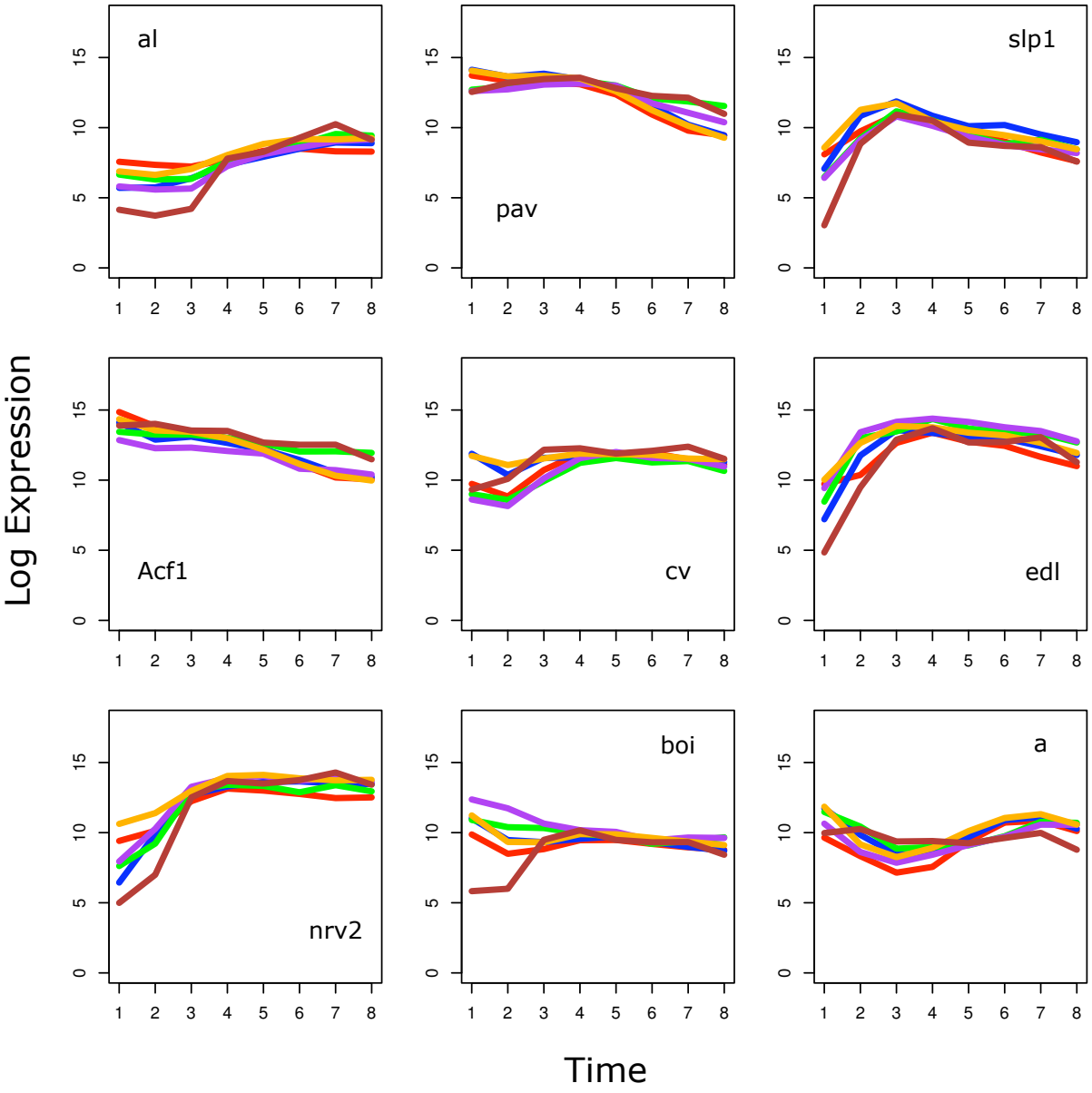

Supplementary Figure 23. A selection of genes that display hourglass divergence profiles chosen so that at least one pair of species has a log_2 fold change of more than 1 at time point 1 and temporal divergence is minimised between time points 3 and 6. Species colours as in Fig. 1.

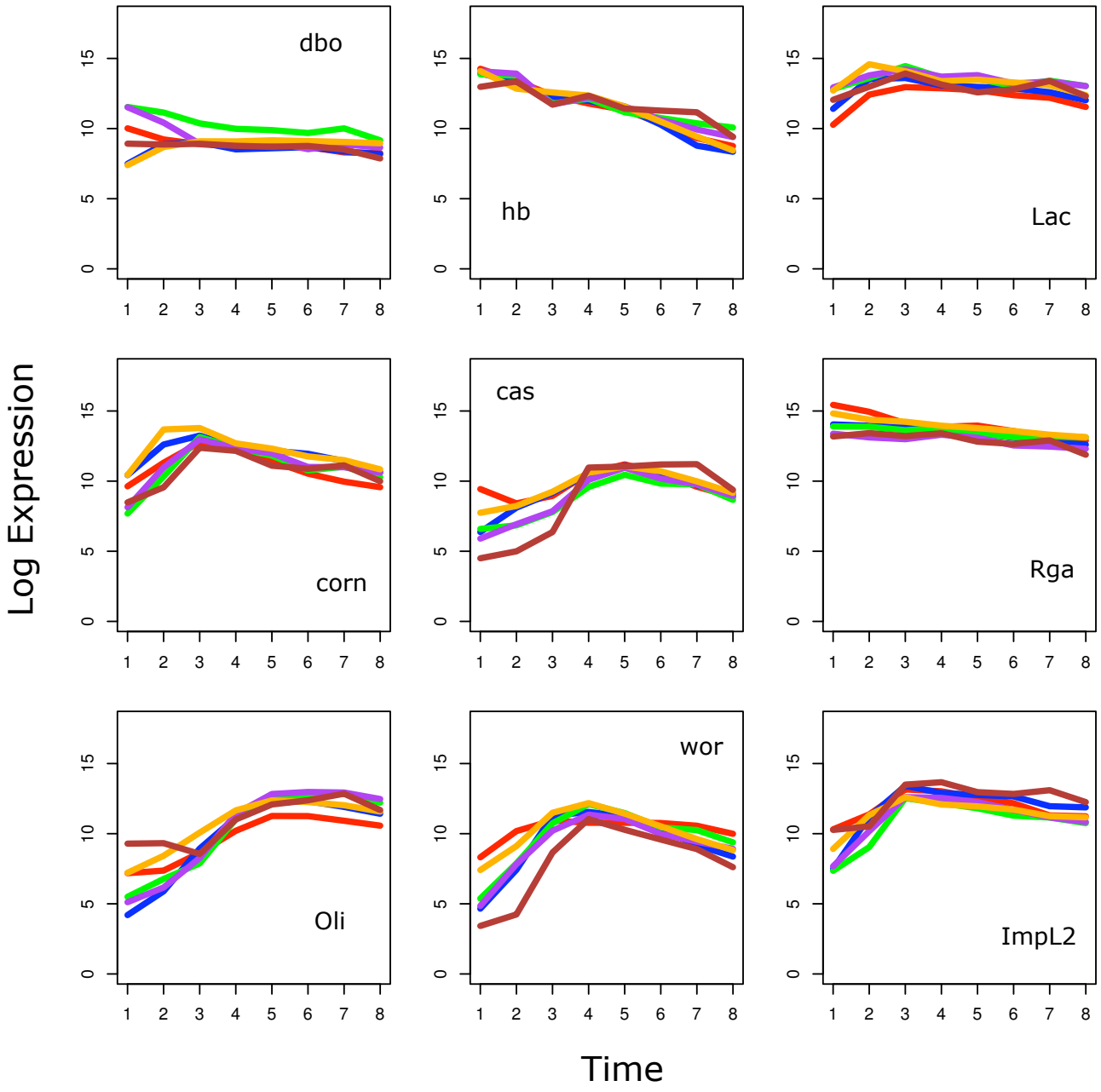

Supplementary Figure 24. A selection of genes that display hourglass divergence profiles chosen so that at least one pair of species has a log_2 fold change of more than 1 at time point 1 and temporal divergence is minimised between time points 3 and 6. Species colours as in Fig. 1.

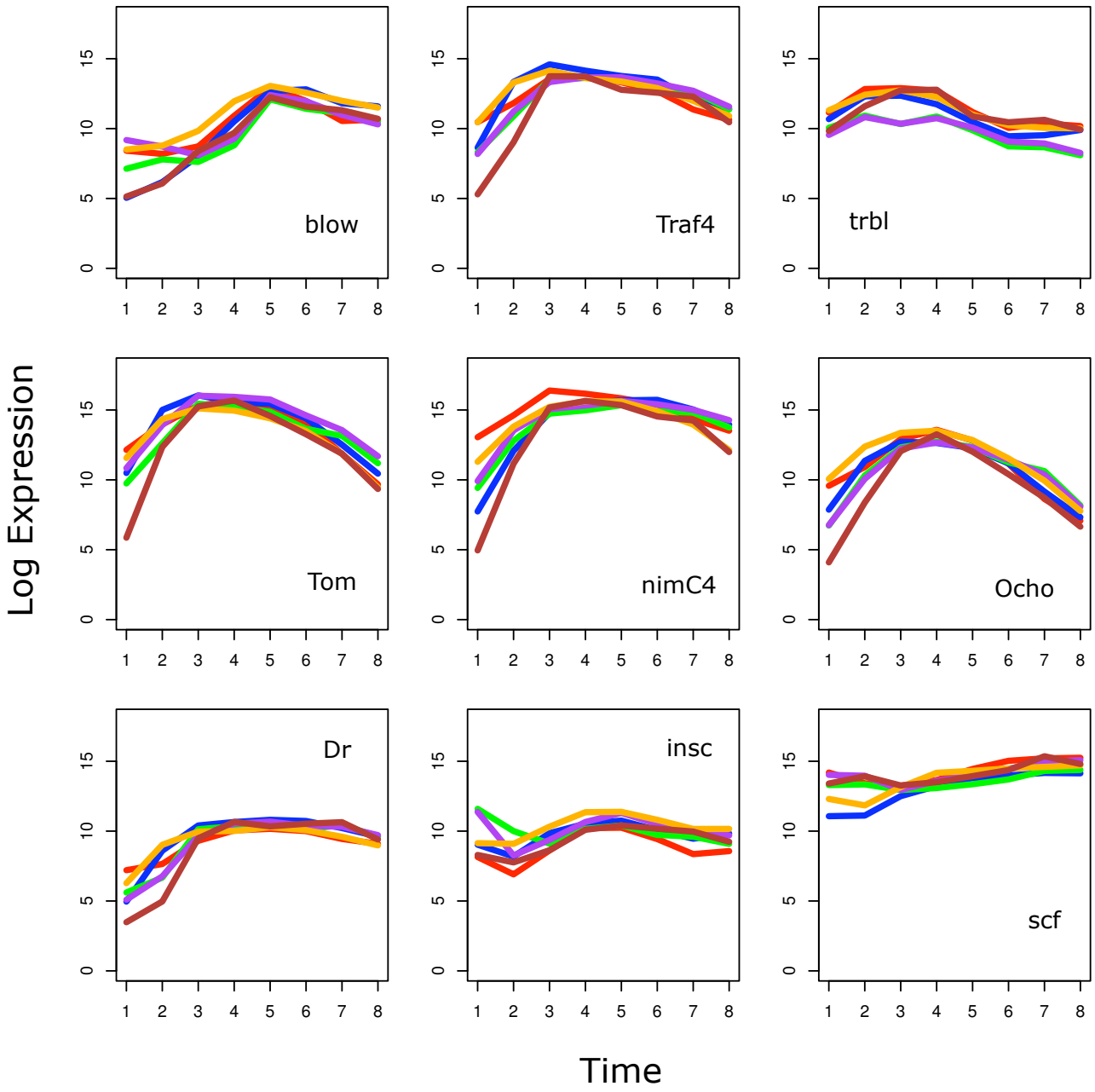

Supplementary Figure 25. A selection of genes that display hourglass divergence profiles chosen so that at least one pair of species has a log_2 fold change of more than 1 at time point 1 and temporal divergence is minimised between time points 3 and 6. Species colours as in Fig. 1.

Supplementary Table 16

Gene Symbol	Gene	Biological Function
al	aristaless	regulation of Notch signaling pathway; regulation of transcription.
pav	pavarotti	smoothened signaling pathway; cell fate determination.
slp1	sloppy paired 1	heart formation; specification of segmental identity.
Acf1	ATP-dep chromatin assembly fac	system development.
cv	crossveinless	positive regulation of muscle organ development.
edl	ETS-domain lacking	regulation of transcription; embryonic pattern specification.
nrv2	nervana 2	open tracheal system development.
boi	brother of iHog	smoothened signaling pathway.
a	arc	compound eye development.
blow	blown fuse	mesoderm development.
Traf4	TNF-receptor-associated factor 4	eye development.
trbl	tribbles	regulation of cell cycle.
Tom	Twin of m4	sensory organ development; Notch signaling pathway.
nimC4	nimrod C4	apoptotic cell clearance.
Ocho	Ocho	sensory organ development; Notch signaling pathway.
Dr	Drop	dorsal/ventral pattern formation; regulation of cell fate specification.
insc	inscuteable	regulation of nervous system development.
scf	supercoiling factor	chromatin organisation; positive regulation of transcription.
dbo	diablo	actin binding.
hb	hunchback	torso signaling pathway; positive regulation of transcription.
Lac	Lachesin	open tracheal system development.
corn	cornetto	microtubule binding.
cas	castor	central nervous system development.
Rga	Regena	regulation of transcription.
Oli	Olig family	regulation of transcription.
wor	worniu	brain development.
ImpL2	Ecdysone-inducible gene L2	cell adhesion.

Biological functions of selected genes that display hourglass divergence profiles in Supplementary Figs 23, 24, and 25. Biological functions taken from GO terms.

2.8 Temporally divergent profile examples

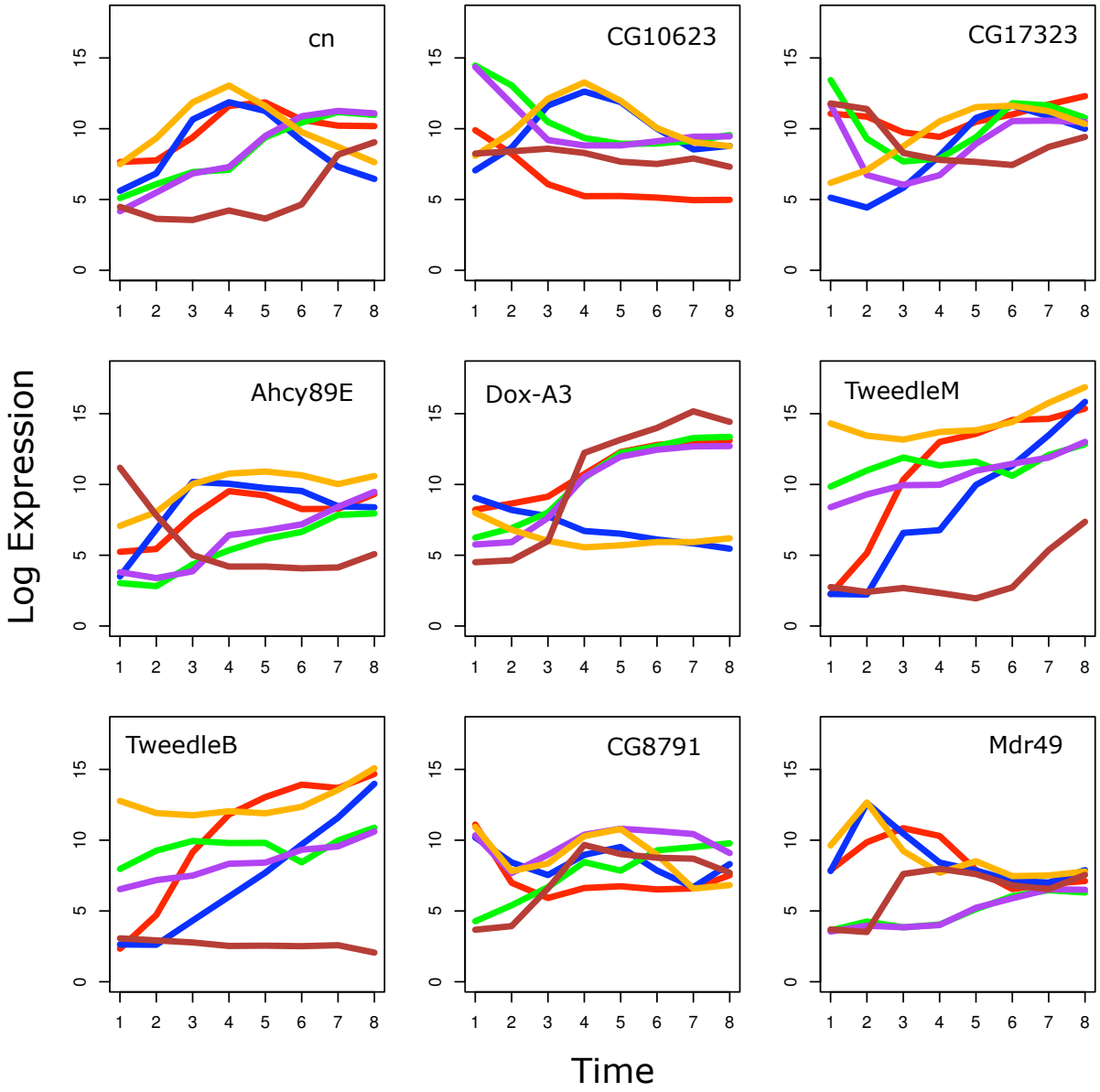

Supplementary Figure 26. A set of genes that have the highest mean temporal divergence in the data set (defined as the highest mean pairwise Mahalanobis distance - see Methods). Species colours as in Fig. 1.

Supplementary Table 17

Gene Symbol	Gene	Biological Function
cn	cinnabar	ommochrome biosynthetic process.
CG10623	CG10623	selenocysteine methyltransferase activity.
CG17323	CG17323	glucuronosyltransferase activity.
Ahcy89E	Adenosylhomocysteinase 89E	one-carbon metabolic process.
Dox-A3	Dopa oxidase-3	NA.
TweedleM	TweedleM	NA.
TweedleB	TweedleB	NA.
CG8791	CG8791	transmembrane transport.
Mdr49	Multi drug resistance 49	response to hypoxia; germ cell migration.

Biological functions of genes with the highest mean temporally divergent profiles in Supplementary Fig. 26. Biological functions taken from GO terms.

2.9 GO analyses

GO analyses of temporal divergence (between-species variance of GST values for each gene) and quantitative divergence (between-species variance of GS values for each gene) shows that metabolic genes are often divergent, whereas housekeeping processes tend to be more conserved (Supplementary Tables 8, 9, 10, and 11). There is a tendency for genes that show strong temporal divergence, such as chitin metabolic genes (Supplementary Fig. 27), to also exhibit somewhat elevated levels of quantitative divergence since genes with dynamically divergent expression patterns may also have differences in their average levels of expression across time. This inertia does not necessarily operate in the opposite direction, however, as it is possible for a gene to be temporally conserved in its expression yet be quantitatively divergent, as shown by the GO term "synaptic transmission" when *D. virilis* is compared with each of the other species (Supplementary Fig. 27).

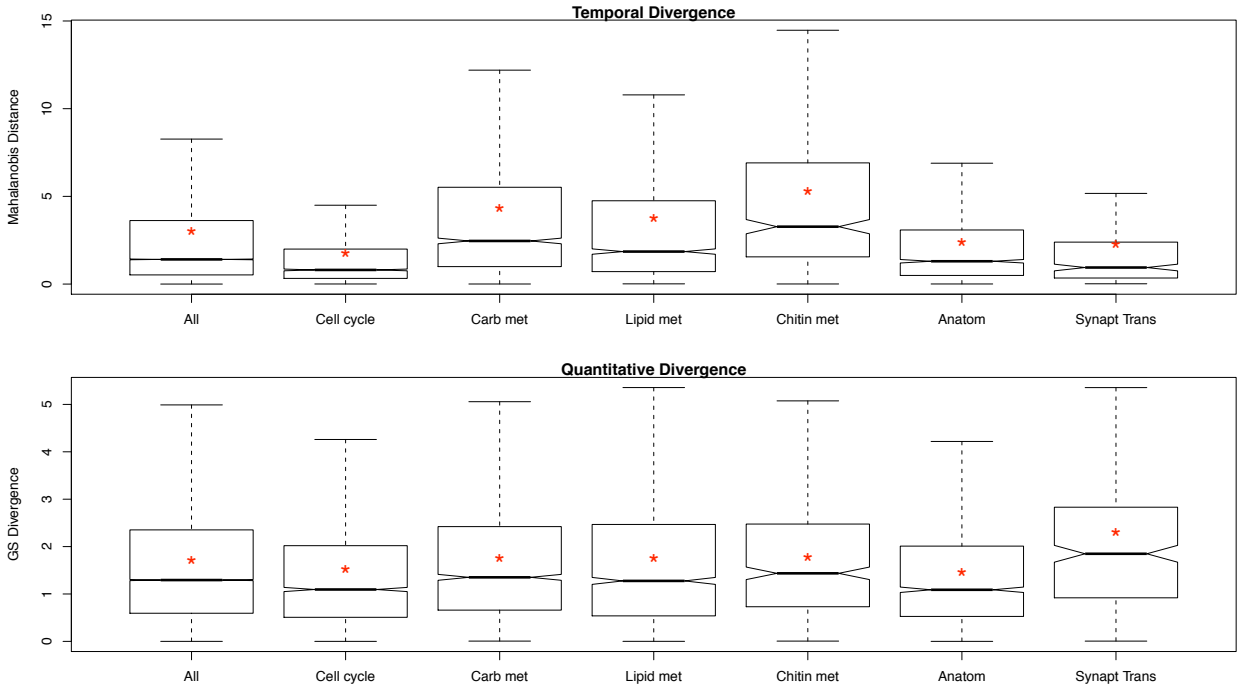

Supplementary Figure 27. Selected GO biological process terms and the divergence measure associated with them (averaged over all pairwise species comparisons per gene). The plots show that temporal and quantitative measures of divergence agree on conservation and divergence across several GO categories. However, certain categories can show temporal conservation but quantitative divergence, such as synaptic transmission, which is measured here for all species against *D. virilis*. Carb - carbohydrate, met - matabolism, Anat - anatomical structure formation, Synapt Trans - synaptic transmission. Red stars indicate the mean. GS divergence refers to t-statistics derived from limma.

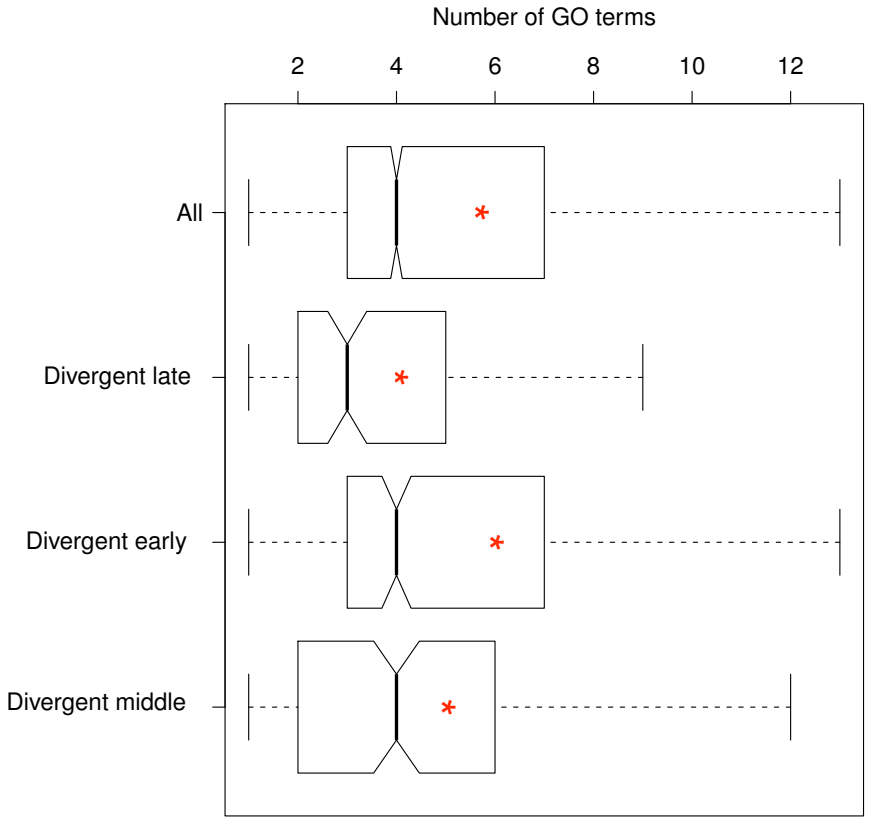

Supplementary Figure 28. The number of biological process and molecular function GO terms annotated to genes that fit different temporal divergence profiles. In each category the top 250 genes are selected and genes without any GO annotations are thrown out. Divergence categories are selected as in Supplementary Fig. 9 (divergence here is relative to the whole divergence profile). The plot shows that genes with increasing divergence profiles (divergent late) have significantly fewer GO terms annotated to them than the global average, which may suggest that these genes engage in fewer interactions. Red stars indicate the mean.

3 Supplementary Discussion

Several studies have explored patterns of evolutionary divergence during embryogenesis in a variety of different species using different measures of constraint. While some morphological studies have found support for the hourglass model [7, 14], studies that have focused on sequency heterochrony have found that there is extensive scope for sequence changes during the phylotypic stage [18,19,59]. The observation that a functional module has been added to the phylotypic stage of zebrafish, most likely under strong selection to avoid predators, suggests that the phylotypic stage may not be immune to novel additions so long as they are modular and do not impact the overall developmental trajectory [62]. Thus, the phylotypic stage in vertebrates may exhibit overall morphological conservation despite the addition of, or even the temporal shifting of, developmental modules whose functional phenotype is limited to later stages of the life-cycle [59].

Genomic and biochemical measures of constraint have also produced contradictory results. Measures of protein distances in vertebrates [15] and dN/dS ratios in *Drosophila* [16,17] have shown a tendency for increased divergence early and late. However, there tend to be more genes with severe loss-of-function and knockout phenotypes expressed early in the development of zebrafish and mouse, with a steady decline towards later periods of development [66] and the coexpression of interacting proteins appears to be most conserved in the early development of the mouse and zebrafish [67]. It has also been observed that gene duplicates tend not to be retained for genes expressed early in zebrafish development [66].

How can we reconcile these observations with our finding that temporal patterns of expression are most conserved during mid-embryogenesis in *Drosophila*? It may be the case that different measures of evolutionary constraint reveal different aspects of the developmental process. For example, while early development may be robust against changes in the expression levels of genes, it may be sensitive to the complete removal of an expressed gene, as is tested by loss-of-function and knockout mutations. Conversely, expression timing during mid-embryogenesis may be important for the correct and optimal development of the organism, but the loss of a gene here may be somewhat compensated by other genes, allowing a non-optimal, yet functional organism to develop. In this case we would expect natural selection to maintain the expression of genes at both stages, but conserve temporal expression patterns more strongly during mid-embryogenesis. Thus, while the mode of early development may be relatively labile, as suggested by several morphological studies [4–7,69,70,72,73,75,76], it still acts as the foundation of the building and requires its processes to be executed in some manner, but may not be sensitive to exactly *how* these processes are executed. It may also be the case that there are less selective opportunities

available for the retention and divergence of function of gene duplicates during the undifferentiated and simple environment of the early embryo relative to later more complex periods.

A recent study of evolutionary constraint in the metabolic network of *Drosophila* showed that enzymes that share metabolites with many other enzymes were constrained, but that this constraint was a function of the topology of the metabolic network as opposed to the essentiality of the enzymes [77]. This result suggests that network topology may be a better predictor of evolutionary constraint than the essentiality of individual network components.

These considerations suggest the type of experimental data that are needed to explore selective constraints acting during embryogenesis. If genes expressed early are more robust against small changes in either their coding sequence or their expression patterns than genes expressed in mid-embryogenesis, then we would expect to see significant differences in the distribution of fitness effects resulting from random mutations of these genes and their *cis*-regulatory regions [78]. Even if the mutational effects are too small to measure, patterns of polymorphism within species will enable fitness effects to be inferred provided large enough sample sizes are taken [78]. Thus, what is required is a fine-grained dissection of mutational effects at each stage of embryogenesis which can then be interpreted together with more coarse-grained loss-of-function and knockout mutations.

It is also possible that fundamental differences between phyla prevent direct comparisons of the constraints acting in vertebrates and arthoropods. A recent study of the regulatory regions of maternal and zygotic genes across different animal species shows that there is a positive correlation between the amount of nutrition provided to the embryo by the mother and the complexity of maternal expression [79]. This means that oviparous species have less specific maternal expression than viviparous species, suggesting that very different constraints may be operating on the early developmental stages of these groups of animals. It has also been shown recently that the pupal stage of the *Drosophila* life-cycle suffers less hybrid misexpression of gene transcripts than larval or adult stages suggesting that the pupal stage is more evolutionarily conserved [29]. Again this suggests that the particular life-history details of different groups of species can significantly impact observed patterns of conservation and divergence.

4 Supplementary References

53. Tweedie, S. *et al.* FlyBase: enhancing *Drosophila* Gene Ontology annotations. *Nucleic Acids Res.* **37**, D555–D559 (2009).

54. Nelson, C. E., Hersh, B. M. & Carroll, S. B. The regulatory content of intergenic DNA shapes

genome architecture. *Genome Biol.* **5**, R25 (2004).

55. Vinogradov, A. E. Compactness of human housekeeping genes: selection for economy or genomic design? *Trends Genet.* **20**, 248–253 (2004).

56. Kristiansson, E., Thorsen, M., Tams, M. J. & Nerman, O. Evolutionary forces act on promoter length: identification of enriched *cis*-regulatory elements. *Mol. Biol. Evol.* **26**, 1299–1307 (2009).

57. Galis, F. & Metz, J. A. Testing the vulnerability of the phylotypic stage: on modularity and evolutionary conservation. *J. Exp. Zool.* **291**, 195–204 (2001).

58. Schmidt, K. & Starck, J. M. Developmental variability during early embryonic development of zebra fish, *Danio rerio*. *J. Exp. Zoolog. B Mol. Dev. Evol.* **302**, 446–457 (2004).

59. Richardson, M. K. Heterochrony and the phylotypic period. *Dev. Biol.* **172**, 412–421 (1995).

60. Richardson, M. K. *et al.* There is no highly conserved embryonic stage in the vertebrates: implications for current theories of evolution and development. *Anat. Embryol. (Berl)* **196**, 91–106 (1997).

61. Bininda-Emonds, O. R. P., Jeffery, J. E. & Richardson, M. K. Inverting the hourglass: quantitative evidence against the phylotypic stage in vertebrate development. *Proc. Biol. Sci.* **270**, 341–346 (2003).

62. Virta, V. C. & Cooper, M. S. Ontogeny and phylogeny of the yolk extension in embryonic cypriniform fishes. *J. Exp. Zool. B Mol. Dev. Evol.* **312B**, 196–223 (2009).

63. Hazkani-Covo, E., Wool, D. & Graur, D. In search of the vertebrate phylotypic stage: a molecular examination of the developmental hourglass model and von Baer's third law. *J. Exp. Zoolog. B Mol. Dev. Evol.* **304**, 150–158 (2005).

64. Davis, J. C., Brandman, O. & Petrov, D. A. Protein evolution in the context of *Drosophila* development. *J. Mol. Evol.* **60**, 774–785 (2005).

65. Cruickshank, T. & Wade, M. J. Microevolutionary support for a developmental hourglass: gene expression patterns shape sequence variation and divergence in *Drosophila*. *Evol. Dev.* **10**, 583–590 (2008).

66. Roux, J. & Robinson-Rechavi, M. Developmental constraints on vertebrate genome evolution. *PLoS Genet.* **4**, e1000311 (2008).

67. Comte, A., Roux, J. & Robinson-Rechavi, M. Molecular signaling in zebrafish development and the vertebrate phylotypic period. *Evol. Dev.* **12**, 144–156 (2010).

68. Sander, K. Specification of the basic body plan in insect embryogenesis. *Adv. Insect Physiol.* **12**, 125–238 (1976).

69. Ballard, W. W. Morphogenetic movements and fate maps of vertebrates. *Am. Zool.* **21**, 391–399 (1981).

70. Wray, G. A. & McClay, D. R. Molecular heterochronies and heterotropies in early echinoid development. *Evolution* **43**, 803–813 (1989).

71. Wray, G. A. & Raff, R. A. Rapid evolution of gastrulation mechanisms in a sea urchin with lecithotrophic larvae. *Evolution* **45**, 1741–1750 (1991).

72. Grbic, M., Nagy, L. M., Carroll, S. B. & Strand, M. Polyembryonic development: insect pattern formation in a cellularized environment. *Development* **122**, 795–804 (1996).

73. Sander, K. Variants of embryonic patterning in insects: Hymenoptera and Diptera. *Semin. Cell Dev. Biol.* **7**, 573–582 (1996).

74. Goldstein, B., Frisse, L. M. & Thomas, W. K. Embryonic axis specification in nematodes: evolution of the first step in development. *Curr. Biol.* **8**, 157–160 (1998).

75. Voronov, D. A. & Panchin, Y. V. Cell lineage in marine nematode Enoplus brevis. *Development* **125**, 143–150 (1998).

76. Chipman, A. D., Haas, A. & Khaner, O. Variations in anuran embryogenesis: yolk-rich embryos of *Hyperolius puncticulatus* (Hyperoliidae). *Evol. Dev.* **1**, 49–61 (1999).

77. Greenberg, A. J., Stockwell, S. R. & Clark, A. G. Evolutionary constraint and adaptation in the metabolic network of Drosophila. *Mol Biol Evol* **25**, 2537–2546 (2008).

78. Eyre-Walker, A. & Keightley, P. D. The distribution of fitness effects of new mutations. *Nat. Rev. Genet.* **8**, 610–618 (2007).

79. Shen-Orr, S. S., Pilpel, Y. & Hunter, C. P. Composition and regulation of maternal and zygotic transcriptomes reflects species specific reproductive mode. *Genome Biol.* **11**, R58 (2010).

80. Artieri, C. G. & Singh, R. S. Molecular evidence for increased regulatory conservation during metamorphosis, and against deleterious cascading effects of hybrid breakdown in *Drosophila*. *BMC Biol.* **8**, 26 (2010).